CLEARINGHOUSE FOR FEDERAL SCIENTIFIC AND TECHNICAL INFORMATION CFSTI
DOCUMENT MANAGEMENT BRANCH 413.11

LIMITATIONS IN REPRODUCTION QUALITY

ACCESSION # AD607157

☒ 1. WE REGRET THAT LEGIBILITY OF THIS DOCUMENT IS IN PART UNSATISFACTORY. REPRODUCTION HAS BEEN MADE FROM BEST AVAILABLE COPY.

☑ 2. A PORTION OF THE ORIGINAL DOCUMENT CONTAINS FINE DETAIL WHICH MAY MAKE READING OF PHOTOCOPY DIFFICULT.

☐ 3. THE ORIGINAL DOCUMENT CONTAINS COLOR, BUT DISTRIBUTION COPIES ARE AVAILABLE IN BLACK-AND-WHITE REPRODUCTION ONLY.

☐ 4. THE INITIAL DISTRIBUTION COPIES CONTAIN COLOR WHICH WILL BE SHOWN IN BLACK-AND-WHITE WHEN IT IS NECESSARY TO REPRINT.

☐ 5. LIMITED SUPPLY ON HAND: WHEN EXHAUSTED, DOCUMENT WILL BE AVAILABLE IN MICROFICHE ONLY.

☐ 6. LIMITED SUPPLY ON HAND: WHEN EXHAUSTED DOCUMENT WILL NOT BE AVAILABLE.

☐ 7. DOCUMENT IS AVAILABLE IN MICROFICHE ONLY.

☐ 8. DOCUMENT AVAILABLE ON LOAN FROM CFSTI (TT DOCUMENTS ONLY).

☐ 9.

PROCESSOR: BM

TSL-107-10 64

OFFICE OF CIVIL DEFENSE

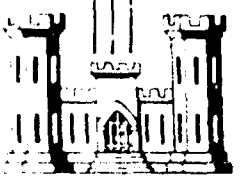

CORPS OF ENGINEERS U.S. ARMY

P.S.D.C. – TR – 14
SEPTEMBER 1, 1964

TECHNICAL REPORT

DESCRIPTION, EXPERIMENTAL CALIBRATION, AND ANALYSIS OF THE RADIATION TEST FACILITY AT THE PROTECTIVE STRUCTURES DEVELOPMENT CENTER

PREPARED BY CONESCO
A DIVISION OF FLOW CORPORATION
CAMBRIDGE MASSACHUSETTS

CONTRACT NO DA–18–020–ENG–3096

PROTECTIVE STRUCTURES DEVELOPMENT CENTER

FORT BELVOIR, VIRGINIA

DESCRIPTION, EXPERIMENTAL CALIBRATION, AND ANALYSIS OF THE RADIATION TEST FACILITY AT THE PROTECTIVE STRUCTURES DEVELOPMENT CENTER

C. McDonnell, J. Velletri
A. W. Starbird, J. F. Batter

Prepared by CONESCO div. of
FLOW Corporation

Contract No. DA-18-020-ENG-3096

Report to

Office of Civil Defense

from

Protective Structures Development Center
Joint Civil Defense Support Group
Office of the Chief of Engineers/Bureau of Yards and Docks

ACKNOWLEDGEMENTS

The authors are indebted to Mr. Sheldon Hunt and Mr. D. S. Reynolds for their untiring efforts in the performance of the experiments described in this report, to Mr. C. Eisenhauer of the National Bureau of Standards for his suggestions and helpful criticisms.

ABSTRACT

The initial calibration experiments performed at the Radiation Test Facility of the Protective Structures Development Center are described and their results analyzed. The dose rate above an open field and the attenuation afforded by the steel frame of the test structure is calculated and found to agree well with experiment when modified calculational procedures are used. The cumulative angular distribution of direct radiation is found to be as much as fourteen percent above that predicted by theory over the range investigated. Several modifications of presently used calculational techniques are suggested.

TABLE OF CONTENTS

TABLE OF CONTENTS (continued)

LIST OF ILLUSTRATIONS

LIST OF ILLUSTRATIONS (continued

LIST OF TABLES

NOMENCLATURE

A	=	Total Area ft.^{2}
A_n	=	Area of n^{th} region ft.^{2}
A_p	=	Perimeter fraction occupied by vertical beams
B	=	Attenuation factor for a vertical slab
B_0	=	Attenuation factor for a horizontal slab
B_1	=	Air ground dose build-up factor - source on ground
B_2	=	Infinite air dose build-up factor
B_3	=	Ground scatter coefficient dose build-up factor
C_g	=	Ground contribution
D	=	Total dose - Roentgens
E	=	Eccentricity factor depending on length to width ratio
E_1	=	Exponential integral of the first kind
F	=	Fraction of infinite field dose
G_a	=	Cumulative angular distribution of 'skyshine' radiation
G_d	=	Cumulative angular distribution of direct radiation
G_s	=	Cumulative angular distribution of wall scattered radiation
h	=	Height of detector ft.
I_o	=	Standard intensity (R/hr) / (Curie/ft^2)
$L(h)$	=	Infinite field dose rate as a function of height
mr	=	milliroentgens
P	=	Atmospheric pressure
	=	Protection factor

Nomenclature (continued)

q_o	=	Specific irradiance (R/hr) / (curie) at one ft.
r	=	Radius
r_i	=	Inner radius
r_o	=	Outer radius
S	=	Source strength
S_w	=	Fraction of radiation scattered by a wall
t	=	Time of exposure - hrs
T	=	Temperature ^{o}F absolute
x_n	=	Thickness of the n^{th} region p. s. f.
x_e	=	External wall thickness p. s. f.
Z	=	Atomic number
σ	=	Density of contamination curies/ft^2
ρ	=	Slant radius, ft.
μ	=	Total cross section (1/448 ft.)
μa	=	Microampere reading of instrument
ω	=	Solid angle fraction = solid and divided by 2π

SUMMARY

BACKGROUND

This report covers the initial program of the Radiation Test Facility and accordingly describes in great detail the physical plan of the test facility, the major items of equipment to be used at the facility, and the various standardization and calibration procedures used to determine the parameters of the present equipment used. Two test series were undertaken in this program. The first series of measurements was directed toward developing a better understanding of the effects of minor variations in the ground smoothness of the test field on the dose rate within the test structure. The second series of tests were directed toward measurements of the perturbations introduced in the radiation field by the steel skeleton supporting the test structures.

RESULTS

The first test series, consisting of the measurement of dose rate above a field contaminated with cobalt-60 of 452 ft. radius, indicated that the departure of the test field from a smooth plane produced only minor variations in dose rate. At the lowermost detector positions of one, three and six feet heights ground roughness caused dose reductions at the center of the test structure of 32, 12 and 3 percent respectively.* A standard value of 464 Roentgens per hour/curie per square foot, three feet above an infinite smooth contaminated plane was determined from these tests and found to agree well with previous measurements. The dose variation with height above the plane showed excellent agreement with that predicted from theoretical procedures developed by Spencer (Ref. 1). The results indicate, however, that the theoretical value of the cumulative angular distribution function for direct radiation, $G_d(\omega, h)$, an important parameter in the computation of the above ground dose rate in a structure, is low by as much as fourteen percent for values of ω greater than about 0.2.

The second series of experiments was directed to determining the perturbations introduced in the radiation field by the steel skeleton of the test structure. It was determined from this series of experiments that with minor modifications, "Engineering

*With reference to the values obtained above an infinite smooth plane.

Manual"[2, 3] type calculations predicted to fair accuracy the effect of the steel frame and the calculated values of $G_d(\omega, h)$ slightly underestimate the true contribution of "direct radiation" for the values of ω, h of these experiments. The azimuthal sector method of accounting for variations in wall mass thickness in the theoretical treatment was found to give good agreement with experiment while the usual technique of mass smearing to handle variations in floor and ceiling structure was found to give poor agreement with experiment. A new technique of summing the area weighted barrier factors for each differential variation in floor and ceiling thickness is proposed. This technique is described by the equation;

$$\overline{B_o(x)} = \sum_{n=1}^{i} \frac{A_n B_o(x_n)}{A}$$

where

$\overline{B_o(x)}$	=	the effective barrier factor introduced by the floor or ceiling
A_n	=	the area of the n^{th} region of floor thickness
x_n	=	the thickness of the n^{th} region of floor thickness
$B_o(x_n)$	=	the barrier factor of a slab of thickness x_n
A	=	the total area of the floor or ceiling

Results of calculations using this technique are found to agree well with the experimental data obtained for both center and off center positions in the steel structure. For practical structures with floor slabs of 40 psf or more the effect of thickness variation might be greatly subdued, consequently, the above technique is not recommended for general use until more realistic structural configurations are studied.

CHAPTER 1

INTRODUCTION

During the past seven years the Office of Civil Defense has carried out continuous research on the problem of shelter from fallout radiation. Part of this research has been directed toward the investigation and development of shelter analysis techniques. Theoretical studies have been performed to provide some understanding of the mechanism of radiation attenuation in complex structures and to develop computational techniques for designing or analyzing structures for their resistance to fallout radiation. Experimental programs have also been performed to evaluate some of the analytical procedures that have been developed, to provide empirical design data for shielding analysis, and to guide the further development of analytical programs and design methods.

These design methods were, for the most part, developed from theoretical data generated by a series of Moments Method and Monte-Carlo style calculations in idealized geometries.[1] The results from the elaborate Moments Method and Monte-Carlo calculations were used to prepare simplified analytical techniques[2, 3, 4] for computing the radiation attenuation afforded by real structures. In the preparation of these techniques, various important assumptions had to be made as to the modes of penetration of radiation and the separability of the geometric and barrier effects on the attenuation of the radiation, and it was important that these assumptions be checked by experiment. Some initial experiments designed for this purpose were carried out on existing structures using cobalt-60 as a fallout simulant. These experiments[5, 6] while extremely fruitful in many respects, indicated the vital need for further experimentation under both simple and complex geometric configurations if an adequate evaluation of the computational procedures was to be made.

During the initial experiments (1958-1961) it was found extremely difficult to obtain access to structures having both the desired geometric features and the prerequisite clearance area for efficient experimentation. In addition, experimentation on such few structures that were available required a "field team" effort that was uneconomical

in light of the general type of data obtained and impractical to maintain on a continuous basis.

As a direct result of these preliminary tests a decision was made to proceed with an investigation of structures of simple geometry using both a scale modeling technique and full scale testing. To eliminate many of the problems associated with full scale testing a test facility was established for performing the detailed experimental evaluation of shielding computational techniques. This report describes this full scale test facility (located at the Protective Structures Development Center, Fort Belvoir, Va.) and the initial "calibration" and standardization experiments that have been performed.

A very detailed description is presented of the test facility, the experimental equipment, and the calibration procedures used. This is done for several reasons. A complete understanding of the equipment and test procedures will allow other investigators to assess the reliability and significance of the data obtained. The equipment and test procedures have evolved during the course of several years work in radiation testing and the specific details may be of interest to other investigators. This is the first test report from the Radiation Test Facility and since much of the data in subsequent reports will depend upon calibration numbers developed in this report, it is important that the calibration results be reported in great detail.

CHAPTER 2

DESCRIPTION OF TEST FACILITY

2.1 GENERAL DESCRIPTION OF THE PHYSICAL PLANT

The Radiation Test Facility of the Protective Structures Development Center is located on a 150 acre site at Fort Belvoir, Virginia, about 15 miles south of Washington, D. C. The complete facility is composed of a test structure, a prepared test site, an operating headquarters bunker, storage buildings, equipment for the simulation of fields contaminated with radioactive fallout, and the associated test and safety instrumentation. This facility was designed specifically to investigate, improve and further develop methods of fallout shelter design. A detailed description of how the design of the test facility was arrived at is found in reference 7.

2.1.1 Test Site

The Radiation Test Facility, which is part of the Protective Structures Development Center, is located together with the Center at Fort Belvoir, Virginia. This location, near Washington, D. C., was chosen so the OCD research personnel may conveniently participate in the planned test programs. The site is a 150 acre rectangularly shaped area with both open and wooded regions. (See Figure 2.1). The test site has a six foot high chain link exclusion fence marking the boundaries of the site. A 500' x 700' test pad, stabilized with washed gravel, is located at the center of the site and is surrounded by a fence marking the boundary of the high radiation area. A controlled access road leads into the site. The test pad is a slightly sloping area pitching down by approximately four feet from the SE to NW corner. This test pad is located such that a minimum of 1,000 feet of clearance exists between the test pad and the outer exclusion fence.

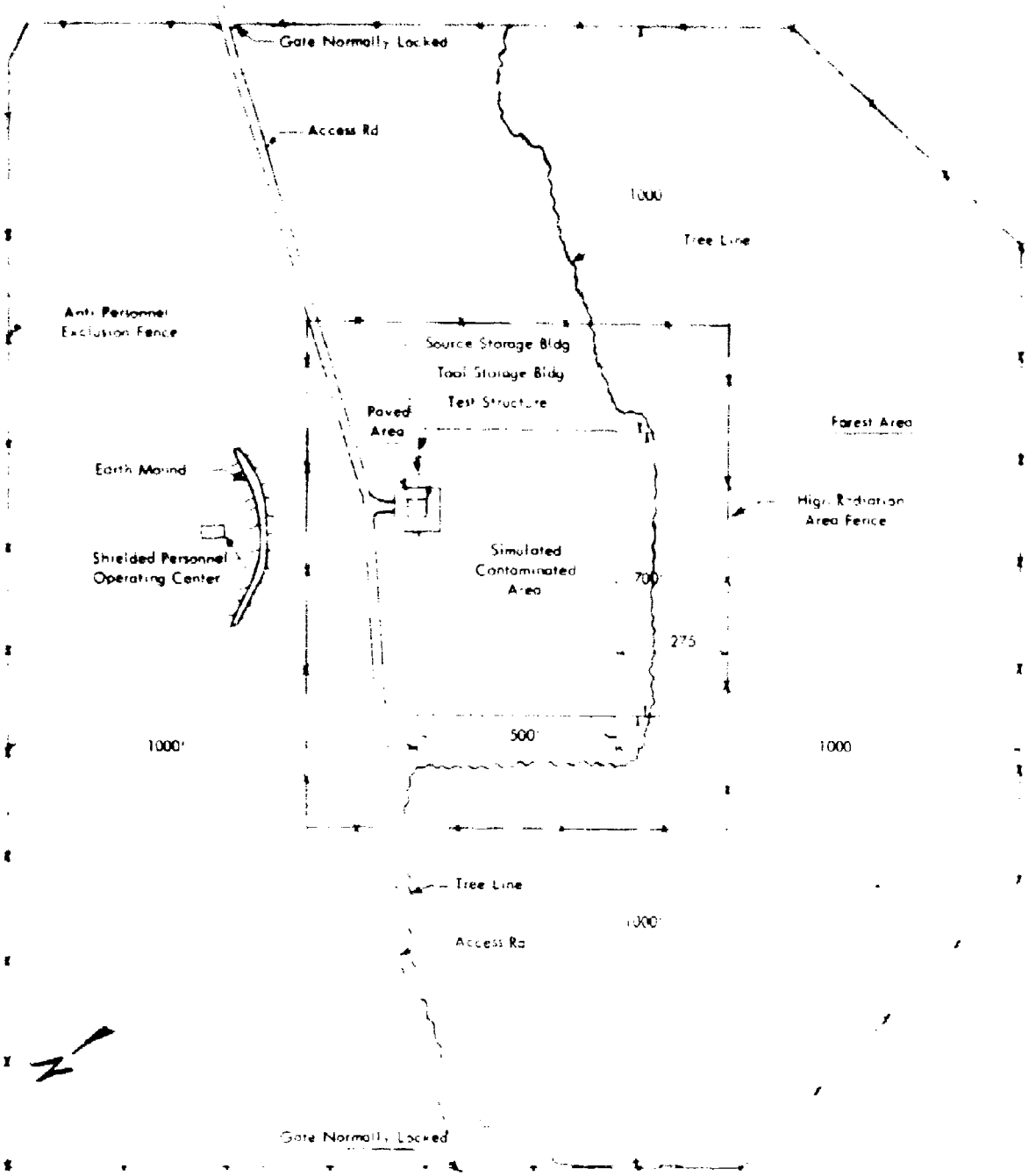

Figure 2.1 - Plan View of Test Site

2.1.2 Test Structure

To facilitate the construction of various types of test structures a 24 ft x 36 ft basement foundation complete with entry way and an above ground steel framework to support the panels of the test structure is located along the southeast edge of the test pad, 200 feet from one corner. The test structure design uses a basic 12 ft x 12 ft module for each of the three above ground floors. Exterior walls and floors of the modules are constructed by placing 4 ft x 4 ft by 4-inch concrete panels in the desired positions. The structure is designed such that walls and floors may be conveniently varied from zero to twelve inch thickness in 4-inch increments. A view of the test structure both with and without concrete panels in place is given in Figures 2.2 and 2.3 respectively.

A crane is required to place each of the concrete panels since they weigh approximately 800 lbs. The area immediately surrounding the test structure is paved to facilitate crane operations.

2.1.3 Outer Exclusion Fence

The outer exclusion fence of the test area (see Figure 2.1) consists of a 6-foot high chain link fence topped with a barbed wire overhang. This fence provides a barrier to the general public and is located to meet the Atomic Energy Commission requirement that a person continuously present at or outside this fence will not receive more than two milliroentgens in any one hour, 100 milliroentgens in any seven consecutive days or 500 milliroentgens in any period of one calendar year. Since planned exposure times at the test facility never exceed 40 hours in any seven day period and since there are no people continuously near the fence (or within several hundred yards of it), the 2 mr/hr limitation was the most restrictive requirement and was used in selecting fence location and source sizes. This fence is marked at distances of approximately fifty feet with signs bearing the radiation symbol and the words "Caution Radiation Area".

A road through the test area, used as access to the radiation facility, required that a gate be placed in the outer fence at two locations. These gates are

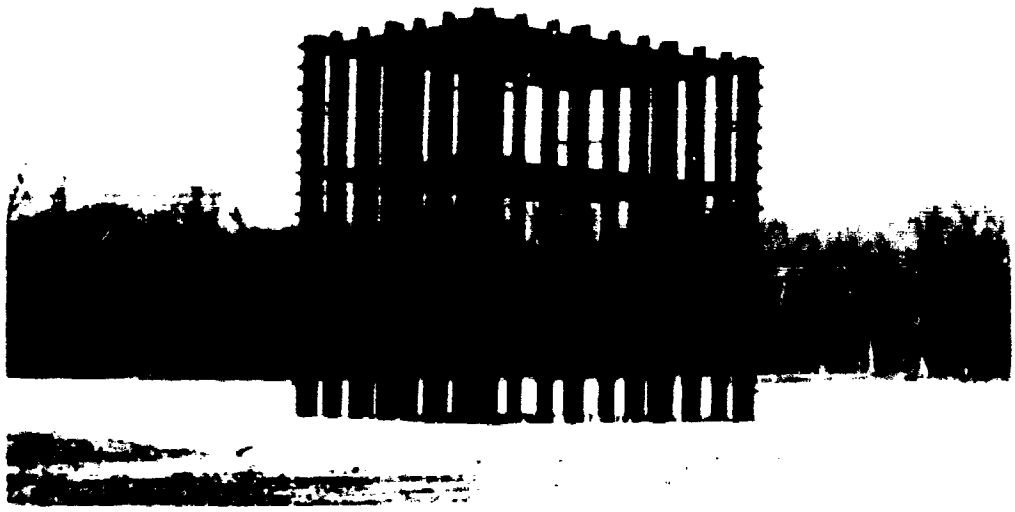

Figure 2. 2 - Skeleton Test Structure without Panels Installed

Figure 2. 3 - Test Structure Illustrating Placement of Wall Panels

normally locked and only approved operating personnel have access to the keys. Each of these gates is marked with warning signs and two flashing red lights. These lights operate only when a source is exposed in the Radiation Test Area. Each gate is also wired so that a loud alarm sounds in the test area whenever a gate is open.

2.1.4 High Radiation Fence

The test facility also contains a 3-foot inner exclusion fence designed to prevent accidental entry into a high radiation field by personnel while a test is in progress. This fence is located such that with the largest test source exposed anywhere on the test pad the dose rate at this fence is below 100 milliroentgens per hour. Signs having the radiation symbol and the words "Caution High Radiation Area" are posted at approximately 100 ft. intervals along this fence.

There are four openings in this fence; two for the road used as access to the test site, and a third and fourth on the driveway and sidewalk leading to the personnel operating bunker. Each of these openings is equipped with a chain for closure and is marked with a "Caution High Radiation" sign. A radiation monitor located within this fence operates an alarm bell which rings continuously during source exposure. This bell is audible at all locations within the high radiation area.

2.1.5 Operating Structures

Three buildings are within the test site. Two of these, located immediately adjacent to the test structure, are used as storage space for equipment and radioactive sources. These two buildings are appropriately marked for such usage by external signs. In addition, a secondary calibration range useful for checking calibrations of both test and survey instrumentation has been constructed in one of these structures. The third structure, which is used as a control building during actual exposure is located approximately 300 feet from the test structure.

The control building is a quonset hut of 20 ft x 20 ft plan area. An earthen mound, approximately 12 feet high has been placed such as to "shadow" the personnel operating bunker from the test area. Personnel may occupy this structure while the largest sources of radioactivity are being exposed in the test area, and receive less

than 2 milliroentgens per hour exposure. This structure also houses the pumping console used for the control of the test sources; thus the console is available to operating personnel at all times during a test exposure so that complete control of source position and velocity is always maintained.

2.2 FACILITY RADIATION CAPABILITIES

The Radiation Test Facility of the Protective Structures Development Center has been established so that tests can be performed upon realistic structures in a simulated fallout environment. The overall radiation capabilities of the facility are determined by the maximum source size usable in the facility and the sensitivity of the radiation detection instruments.

2.2.1 Maximum Source Size

The selection of the proper isotope to use as a fallout simulant was based upon three criteria. First, the attenuation properties of common structural materials for both the selected isotope and actual fallout contamination should be similar; second, theoretical results using identical mathematical procedures based upon the energy spectrum of fallout and that of the selected isotope must be available; and third, the isotope selected must have a long half life, and high specific activity (to reduce self shielding).

The isotope, cobalt-60 has been selected by the staff of the Protective Structures Development Center as most nearly meeting these criteria. This isotope was readily available from normal commercial sources, emits an energy spectrum that well represents that of fallout at early times, and has both long half life and high specific activity. In addition, there was available more theoretical data[1, 2] comparing the effects of cobalt-60 and fallout radiation than for any other isotope.

The limitations placed upon the maximum source strength is set by the fact that the dose rate at the outer exclusion fence must not exceed that specified by the Atomic Energy Commission. Paragraph 20.105 of the Nov. 17, 1960 edition of the Commission's rules states that "no licensee shall... create in an unrestrictive

area... radiation levels... (1) in excess of two millirems in any one hour or (2) radiation in excess of 100 millirems in any seven consecutive days." The first of these two limitations determined the source size.

Since the source must be assumed capable of being placed anywhere on the test pad, (see Figure 2.1) the minimum distance from the source to the exclusion fence was 1000 feet. The maximum allowable source strength computed from the 2 millirems per hour limitation is thus 600 curies of cobalt-60.

2.2.2 Instrument Selection

The estimated attenuation characteristics of the test structures together with the maximum allowable source size sets a lower limit on the sensitivity of the required test instrumentation. The size of the test pad and the location of the test structure within the pad is such that the largest circular field of simulated contamination that can be produced is a quarter circle of 500 feet radius or a semi-circle 200 feet in radius. These fields surrounding the cleared area representative of the structure, if, of full circumference would represent, respectively, approximately 60 percent and 50 percent of the dose rate (at 3 feet height) that would be obtained from an infinite field. The tests described in this study have been carried out with a quarter-circle test sector extending to approximately one mean free path radius (450 ft. in air). This sector was in turn subdivided into four separate concentric annuli each contributing approximately 4% of the infinite field dose rate.

The expected dose rate within the test structure from one of these test annuli can be computed as follows: the simulated source density is equal to the source size, multiplied by the time of exposure, divided by the area over which the source travels. Since an infinite field of one curie of cobalt-60 per square foot density creates a dose rate of 464 R/h, 3 feet above it, the dose accumulated within the test structure during an exposure may be written approximately as:

$$D = \frac{I_o FtS}{AP_f}$$

where D = Total accumulated dose in the structure in roentgens

I_o = Dose rate 3 feet above an infinite field of contamination of one curie/ft^2 cobalt-60 in roentgens/hr

F = Fraction of infinite field represented by the test annulus
t = Time of exposure in hours
S = Source strength in curies
A = Area of the test annulus in ft^2
P_f = Protective factor afforded by the structure from ground based source of contamination

The maximum source size of 600 curies gives a total accumulated dose inside the test structure of about 0.7 mr with a ten hour exposure if the test structure is assumed to have a protection factor of 1000 from ground based sources of radiation (a very high protection factor). This value (0.7 mr), about ten times the natural background dose, is adequate for accurate experimentation. Thus, using this value as a minimum measurement in any experiment, three ionization chamber dosimeters were selected for use. These are the Victoreen Model 208 Chamber of 0-1 mr range; the Victoreen Model 239 Chamber of 0-10 mr range; and the Victoreen Model 362 Chamber of 0-200 mr range.

2.3 SELECTION OF SIMULATED FIELDS OF CONTAMINATION

To simulate an experimental uniform field of contamination it is necessary to utilize equipment which will cause the source to spend the same amount of time in each differential area of the simulated field. The simulation technique used is to pump a sealed source at constant velocity through long lengths of tubing that has been permanently placed at a uniform density over the test area, and to sum the resulting doses at the test locations with integrating type dosimeters. At any location the dose from the entire field is the sum of the dose from all differential areas of the field. These differential doses are summed automatically through the use of detectors that integrate doseage over the total exposure time.

In the design of simulated contaminated areas the approach found most useful in experiments of this type has been to divide the field into several circular annuli surrounding the structure to be tested. Tube spacing and source size can then be varied from annuli to annuli to minimize the amount of tubing and test time required. Circular annuli are generally chosen so as to minimize the effects of source anisotropy.

This anisotropy is partially caused by the column of water which propels the source, attenuating radiation in the fore and aft direction of the source. If circular annuli are chosen such that the source is always side-on to the structure to be tested the radiation seen by the structure is not affected by this water column. Each annuli is sized to represent approximately the same fraction of total infinite field ground dose. These annuli extend from the base of the structure to a distance of about one mean-free path from the structure. Since in an infinite field the dose originating from contamination within this area creates over 90 percent of the total dose for moderate detector heights, a contaminated test area of this size is well representative of the infinite field.

With respect to the test structure the energy spectra and angular distribution of radiation originating from sources lying at distances in excess of approximately ten building heights or one mean free path distance (whichever is greater) is approximately unchanged. Hence, the outermost annuli of the contaminated area of the described test field is representative of "far field" contamination and is useful for making analytical estimates of radiation dosage that would emanate from sources lying in this "far field" region.

The fraction of infinite field dose rate obtained from a circle of contamination of given radius is illustrated in Figure 2.4 for both the conventional 3 ft. height, and at 56 ft., the maximum height of the proposed test structure. The test field extends from the base of the structure (external dimensions 26.3 ft x 38.3 ft) to a radius equivalent to one mean-free-path for cobalt-60 radiation (450 ft.). Past experiments in tests of this type indicate that a division of the simulated field into four annuli areas is useful for the interpretation of the results obtained. The inner and outer radius of each annulus of contamination was thus chosen so that each annulus represented approximately the same fraction of infinite field dose (within the limitations imposed by ease of placing the test tubing within each area).

Since the test building is rectangular in shape, representing a cleared area of 26.3 feet by 38.3 feet, for computational purposes the equivalent inner radius of the innermost annulus was assumed to be 17.9 ft., the radius of a circle that contained the same area as the rectangular structure. The total area of simulated

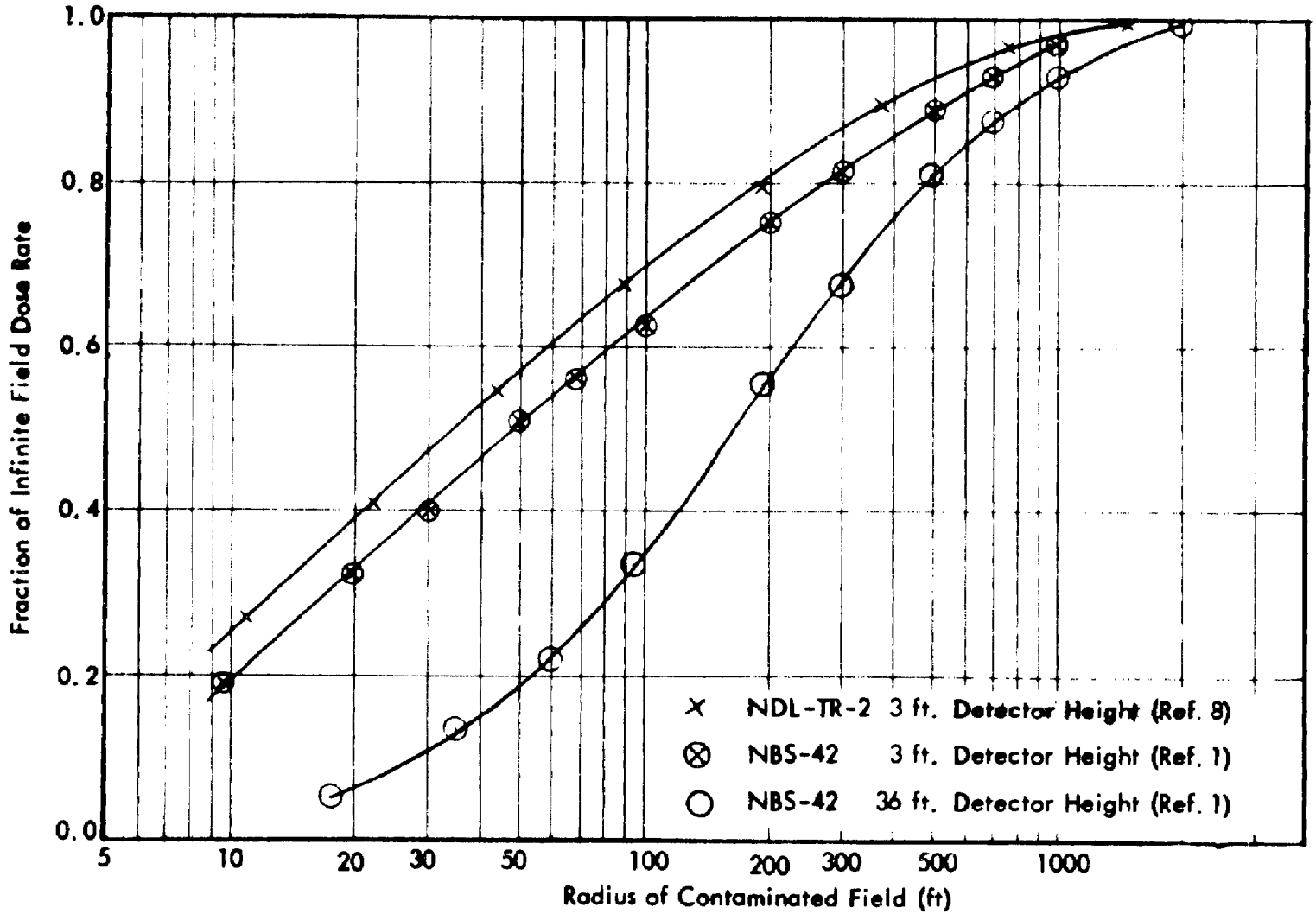

Figure 2 4 - Dose Rate at the Center of a Contaminated Circle as a Fraction of Infinite Field Dose Rate

ground sources of contamination thus extends from 17.9 feet to 450 feet radius. This area (see Figure 2.4) represents 55 percent of the infinite field dose at a 3 ft. detector height. Each annulus is sized to represent approximately 13.75% of the infinite field ground dose. Using the inner radius of 17.9 feet for area 1, the outer radius for this area required to give 13.75% of the infinite field value at 3 feet height is approximately 33 feet as determined from Figure 2.4. Approximate radii for areas 2, 3, and 4 were determined in a similar manner (see Table 2.1).

TABLE 2.1

APPROXIMATE RADII OF ANNULAR FIELDS OF CONTAMINATION YIELDING EQUAL FRACTIONS OF INFINITE FIELD DOSE RATE

AREA	INNER RADIUS (ft.)	OUTER RADIUS (ft.)
1	17.9	33
2	33	75
3	75	170
4	170	450

The total area of a circular field of one mean-free-path radius is approximately 640,000 square feet. Since it is generally desirable to limit the maximum spacing of the tubing through which the source travels to one-third or one-quarter of the vertical size of any aperture in the structure, especially near the test structure, a large amount of tubing is required. Use is made of the symmetry of the test structure, wherever possible, to reduce the total amount of tubing. Since the test structure proposed for the first several series of experiments was rectangularly symmetrical, it was possible to represent a complete field of contamination by simulating contamination in only one quarter of the field and by using symmetrically located radiation detectors in the test structure to account for the full field. The radii of the fields have been modified slightly from those of Table 2.1 to accommodate tube spacing of 1, 2, 4, and 16 feet. The detailed characteristics of each of the test areas including the amounts of tubing used, etc. is presented in Table 2.2.

TABLE 2.2

THE CHARACTERISTICS OF QUARTER SYMMETRICAL EXPERIMENTAL CONTAMINATED AREAS
(Based on Data of References 1 and 8)

Area No.	Inner Radius (ft.)	Outer Radius (ft.)	Tube Spacing (ft.)	Area $(ft.)^2$	Approx. Length of Tube (ft.)	percentage of Infinite Field Dose Rate		
						3 ft. height		36 ft. height
						NDL-TR-2	NBS-42	NBS-42
0	-	17.9*	-	-	-	9.40*** / 9.09**	7.29**	1.10**
1	17.9	32	1	552	550	2.92*** / 3.23**	3.0 **	0.94**
2	32	68	2	2,828	1,400	3.45	3.62	1.78
3	68	164	4	17,492	4,400	3.75	4.10	4.05
4	164	452	16	139,357	8,700	3.53	3.87	3.61

* Equivalent radius; actual area rectangular in shape 26.3 ft x 38.3 ft

** Based on equivalent radius of 17.9 ft.

*** Based on rectangle area of 26.3 ft x 38.3 ft.

As the major purpose of the first series of building experiments was to test the effect of structural variations only rather than the combined effect of the ground and the structure, a "free field" test, i.e., with no building present, was required to evaluate the effect of ground roughness. Ideally this test would be conducted with the contaminated areas surrounding the test structure site before the structure was installed. This was impossible, however, as the permanent steel frame of the structure was already in place in advance of the experimental effort. Since the ground surrounding the test structure was a smoothly graded rectangular field covered with gravel, and since this field upon physical inspection appeared quite uniform in its deviation from perfect smoothness throughout its area, it was thus decided to evaluate the entire test field for the effects of ground roughness by using duplicate contaminated areas offset 75 feet to one side of the test structure.

2.4 DETAILED DESCRIPTION OF CONTAMINATED AREAS

The area of "fallout" simulation for the "open field" experiments and skeleton structure are identical. Each consist of a quarter circle field 452 feet in radius. This field is broken into five individual areas as shown in Figure 2.5. To differentiate between these, the areas surrounding the test structure are labeled 1, 2, 3, and 4 and those surrounding the open field 0A, 1A, 2A, 3A, and 4A respectively.

The first of these areas (Area 0) is rectangular in shape and is identical in size to the outside dimensions of one quadrant of the "skeleton" structure (13' 2" x 19' 2"). Tubing for this area was required only for the open field experiment and was layed with parallel straight runs of tubing at a one foot spacing. The tubing leads between the source container and area 0A were long enough (relative to the total length of tubing in the area) to require shielding with 8 inches of concrete block. This shielding was selected to reduce the dose contribution from the source while it is in the leads to and from the test area to less than one percent of that measured in the experiment. Area 1 contains a transition from the rectangular shape of Area 0A to the circular geometry of areas 2, 3, and 4. The tubing for area 1 was arranged in a rectangular pattern except for the region at the outermost edge of the area where the

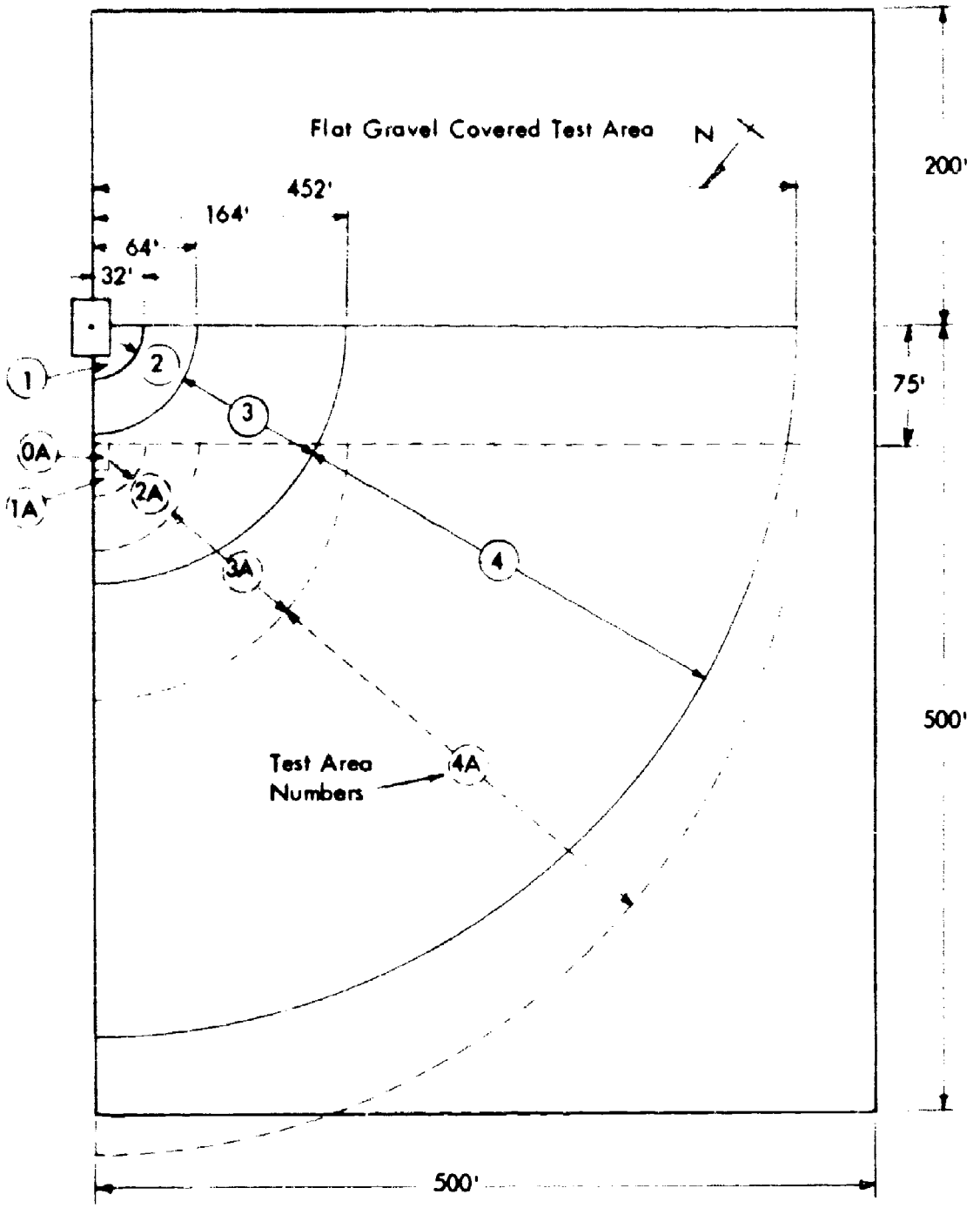

Figure 2.5 - Plan View of the Test Areas

transition to a circular pattern was made. Care was taken to fill this region to the same tubing density as existed in the inner part of this area. Areas 2, 2A, 3, 3A, 4 and 4A were circular annuli and tubing was positioned in a circular array. Dimensions, area, spacing, tubing length and percent of infinite field dose rates for those fields were previously given in Table 2.2 Tubing leads from each area were terminated at a concrete walkway paralleling one side of the simulated source field. Lead length required to connect each area to a source container located on the walk was about 10 feet. The leads for areas 0A, 1, 1A, 2, 2A, 3, 3A were located at the outer radius of each area to keep extraneous dose contributions at the dosimeter positions to a minimum. In area 4 and 4A, however, since the length of the leads were a small fraction of the total tubing, the leads from the source container to the tubing area were positioned at the inner radius This gave a significant reduction in the length of the pump to source container tubing.

2.5 SOURCE CIRCULATION SYSTEM

A uniform source density was simulated in each test annuli by circulating a sealed source of radioactive cobalt-60 at constant velocity through a large loop of tubing uniformly placed in the particular test area of interest. Three sources of approximately 6, 60, and 600 curies strength were available for these tests. In operation, the source was forced through 3/8 inch I.D. polyethylene tubing using a water-antifreeze mixture as the propelling fluid. A schematic diagram of the hydraulic system used for circulation of the source is shown in Figure 2.6. The propelling fluid is drawn from a reservoir into the appropriate pump or pumps and then forced through the source container. This operation drives the source assembly out of its storage position in the container, through the loop of polyethylene tubing representing the area of contamination to be simulated, and then back to the storage container at the conclusion of the exposure.

2.5.1 Pumping Console

The source pumping console consists of two pump assemblies, a storage reservoir, and valves for controlling fluid flow to the source storage container and the polyethylene tubing in the test area.

A picture of the pump console is given in Figure 2.7. The primary pump

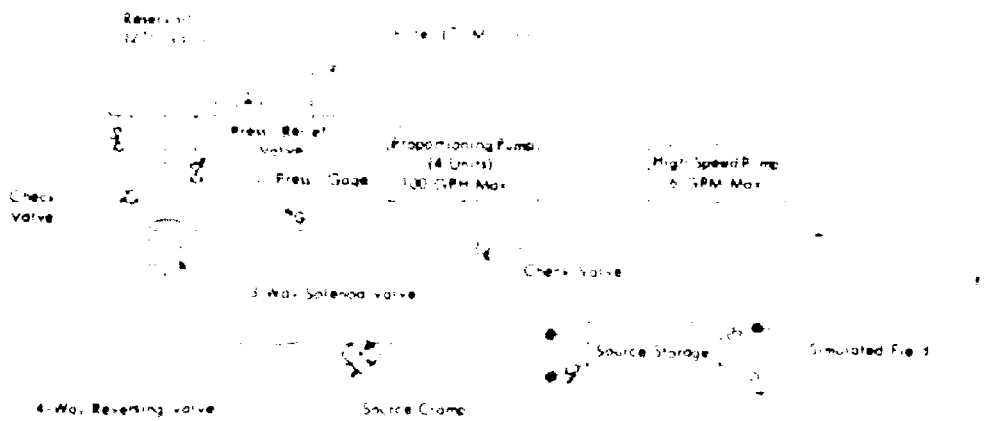

Figure 2.6 - Diagram of Hydraulic Source System

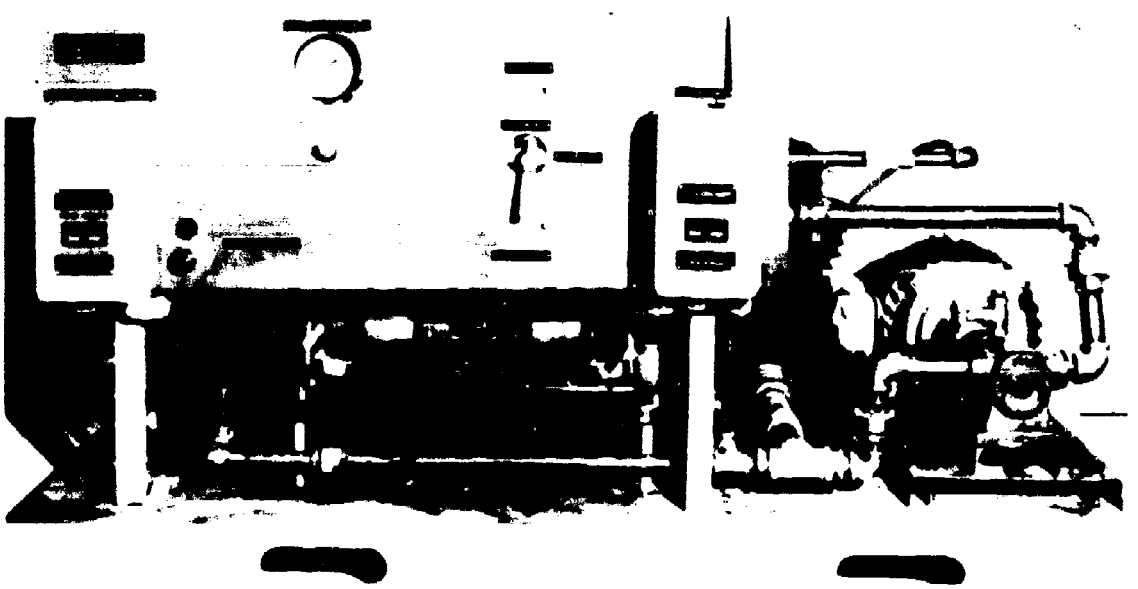

Figure 2.7 - Pumping Console

assembly is a four-feed Hills-McCanna positive displacement proportioning pump. The drive for this pump consists of a 3/4 hp, 220 volt, 3-phase electric motor coupled to a Vickers variable-speed hydraulic drive and a 23:1 Bison gear reducer. Each of the four pump feeds has a 27 gph maximum capacity and a 200 psi pressure rating. The four feeds are mechanically driven such that their output is staggered by 90 degree increments, thus reducing any pump pulsations to negligible amounts. The unit has been designed to keep output pulses small in order to minimize their effect on source assembly motion. This, together with the "smoothing" effect of the elasticity of the pump piping and lead polyethylene tubing, is such that the source motion is essentially uniform and there is only extremely small changes in differential velocity.

A 10:1 variation in total pump output can be achieved through the use of a Vickers variable speed drive unit. Additional variation in pump output can be obtained by changing the length of the piston stroke of each feed through use of a micrometer adjustment. Details on calibration of this pump assembly are given in Appendix 1.

The second unit of the pumping console is a six GPM Viking Gear pump driven by a 2 hp, 220 volt, 3 phase electric motor. This pump serves as a high-volume pump for rapid source movement or for filling of the tubing circuits. It also serves as a backup unit in case of failure of the primary pumping system. Output from the pump or pumps passes through a 3-way solenoid-operated-valve which allows either for by-passing of the fluid to the storage reservoir or for passage to the source storage container where it will propel the source through the tubing circuit. This solenoid is operated with a keylock switch and remains in the bypass position until the proper key is inserted into the lock and turned to divert flow to the source container. As an additional safety feature a green light (wired to the key lock switch) is "on" whenever the solenoid valve is in the bypass position. Output of the pumping system is monitored by a pressure gauge at all times. In addition, there is provided a pressure relief valve to limit system pressure to 200 psi and a 4-way manual reversing valve to permit the operator to easily reverse the direction of fluid flow and source motion.

2.5.2 Tubing and Fittings

A total of approximately 36,000 feet of tubing was required to properly

cover the test areas. This tubing was prepared in 6,000 ft. le ths to the following specification:

Material – Polyethylene with 0.25 percent C / SORB UV-531 additive
Outer Diameter 0.625 + 0.020 inches
Inner Diameter 0.375; + .005, - .000, inches
Circularity and Concentricity ± .010 inches

Each length was wound on a suitable reel. Figure 2.8 illustrates a reel of this tubing together with the portable reel stand. The tubing contains 0.25 percent American Cyananid CYASORB UV 531 to lengthen its life by decreasing the damage resulting from exposure to sunlight. The ultraviolet portion of the light spectrum causes aging in untreated polyethylene which results in brittleness. The UV 531 additive acts as a screen to filter out the ultraviolet portion of sunlight in the extreme outer layer of the tubing; thus the damage or aging effects are limited to the extreme outer layer of the tubing. The tubing as extruded is quite clear so that the source motion can be observed, and it can be bent into a 6-inch radius without collapsing. This permits unrestricted source assembly passage at low source velocities at this small radius.

Special stainless steel fittings are used to couple together the pump console, source container, and tubing making up the simulated fields of contamination. These fittings use a rubber O-ring seal and have a tongue and groove design for positive alignment. The inner diameter of the tubing circuit is thus free of any discontinuities that might interfere with the free passage of a source assembly.

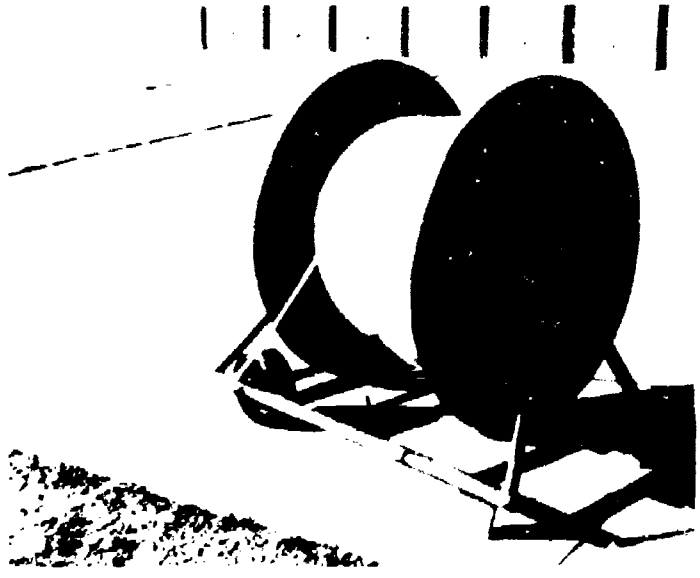

Figure 2.8
Polyethylene Tubing - Tubing Reel and Stand

2.5.3 Source Assemblies

Three source assemblies were used during the test portion of the program. A typical assembly is illustrated in Figure 2.9 and 2.10. The three assemblies were loaded with approximately 6, 60, and 600 curies of cobalt-60 respectively. Each assembly was accurately calibrated prior to usage to determine its actual strength (See Chapter 3).

Each source assembly consists of an encapsulated Co-60 source attached to a hydraulic piston by a length of flexible cable. A piston leather on the forward end of the assembly serves as a seal so that water pumped through the source container will force the piston and the attached source capsule out of the container and through a loop of tubing. The active portion of the source consists of Cobalt-60 pellets encapsulated in a 5/16 inch diameter stainless steel cylinder. The source capsule is attached to the chrome plated carbon steel piston with a 19-inch length of 1/8 inch diameter stainless steel Teleflex cable. This arrangement permits clamping the source assembly in a safe position whereby the active portion of the source is at the center of the storage container while the piston section protrudes outside of the shield; this permits easy inspection, installation, and maintenance of the piston leather.

2.5.4 Source Containers

The three Co-60 sources designed for pumping through the 3/8 inch polyethylene tubing are contained in two identical portable containers, (See Figure 2.11). Each of the two containers has a capacity of 2,000 curies of Co-60 and can normally hold two sources. A container consists of a lead-filled steel shell mounted on two 12 inch solid rubber tires so that it can be moved with the aid of a "skid" spotter. Two pairs of curved 3/8 inch I.D. stainless steel tubes, designed to house the active source assemblies, pass through the container near its center. A clamp at one end of each tube locks the source assembly such that the active portion of the source capsule is located at the center of the container. This clamp is retracted just prior to pumping a source out of its container. Fittings on the end of the storage container tubes match those on the test loops of polyethylene tubing and those on the pumping system. Storage

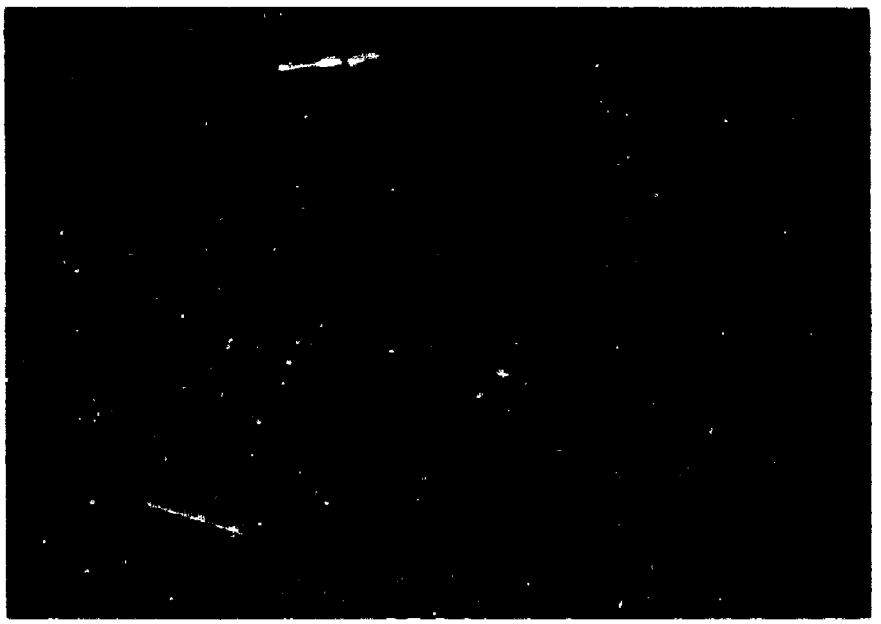

Figure 2.9 - Source Assembly

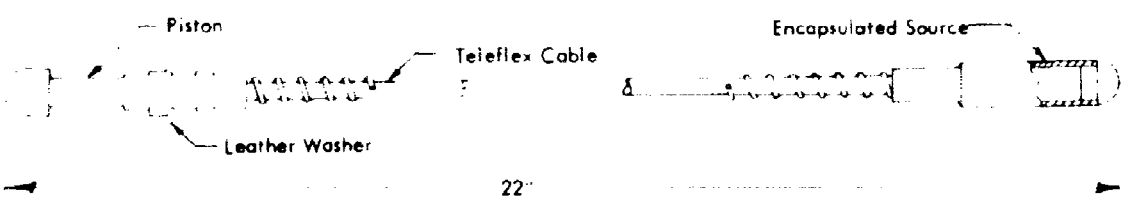

Figure 2.10 - Sketch of Source Assembly

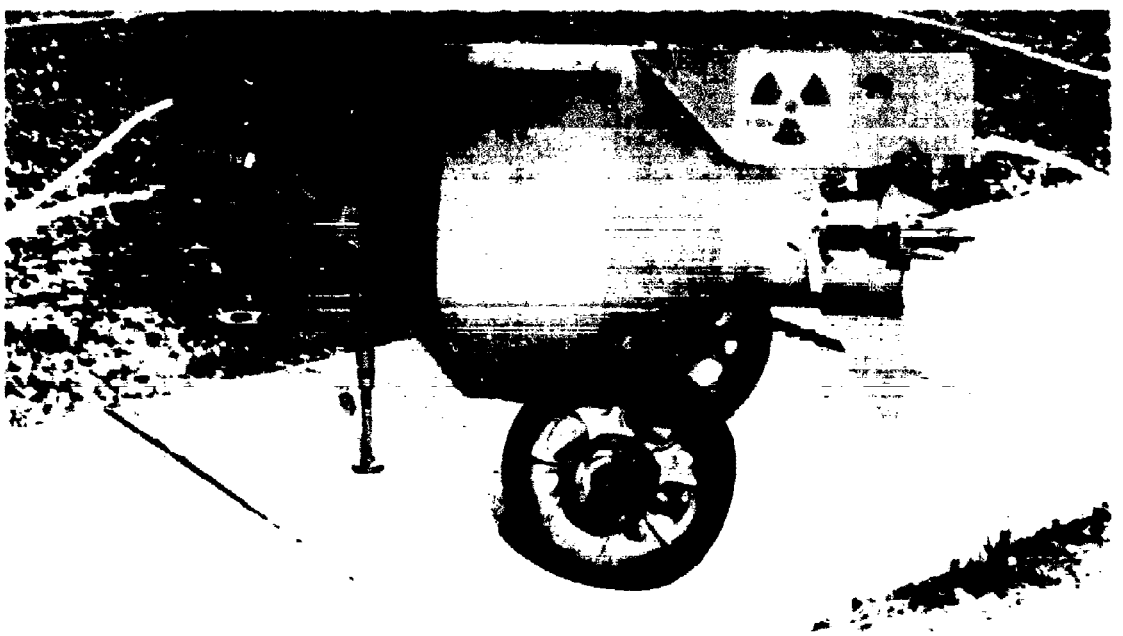

Figure 2.11 - Source Storage Container

plugs threaded to match the end fittings of the source tubes keep the sources positioned at the center of the container when a source is not in use. Each of the storage plugs are designed for locking in position with a padlock.

During operation the source is pumped out of the container, through the tubing positioned in the field, and back to the container. A longitudinal hole (normally plugged) near the center of the lead container allows the tubing itself to be drawn through the container so that in the event a source becomes stuck in the tubing, the tubing can be drawn through the container until the "stuck" source is properly shielded. Each of these containers weighs approximately 3000 pounds.

2.5.5 Emergency Source Container

An emergency source storage container is provided for use in the unlikely event that a source escapes from the tubing. A picture of this container is shown in Figure 2.12. The emergency container consists of a 19 inch diameter lead-filled steel shell, mounted on wheels and weighing approximately 3000 pounds. In the event

Figure 2.12 - Emergency Source Storage Container

of a source escaping from the tubing, it can be picked up with a magnet attached to the center of a long line and dropped into the emergency container. For this purpose the piston end of the source assembly is of magnetic chrome-plated carbon steel while the rest of the assembly is of non-magnetic stainless material. A detachable brass funnel mounted on top of the emergency container facilitates dropping the loose source assembly into the container. A stop in the vertical source receiving tube of the container properly positions the source at the center of the emergency shield while a clamp at the top of this tube permits clamping a source assembly in the shielded position. The source tube has fittings at each end for coupling to the hydraulic pumping system to allow transfer of a source assembly from the emergency container to its regular storage container. Permanent storage plugs are also provided for the unit.

2.5.6 Radiation Instruments

Two kinds of instrumentation were used in this test series, non-direct reading ionization chambers for obtaining experimental data and health physics type instruments for survey and monitoring purposes. Victoreen Model 362 ionization chambers

of 0-200 mr range, Model 239 chambers of 0-10 mr range and Model 208 chambers of 0-1 mr range were used in appropriate locations to gather fundamental data. To prevent electron penetrations the Model 208 chambers were covered with an 1/8 inch thick plastic equilibrium sleeve. These detectors were charged and read with the Technical Operations Model 556 battery operated Portable Charger-Reader. Details of the selection and calibration of these instruments are given in Chapter 3 of this report. In addition to the instrumenrs used in routine test work, a Victoreen Model 570 R-meter with two 0.25 and two 2.5 Roentgen ionization chambers, calibrated by the National Bureau of Standards, was used for instrument and source calibrations.

Personnel monitoring was performed with three Victoreen Model 592 B survey meters having a range up to 1000 mr/hr in three steps: 0 to 10 mr, 0 to 100 mr and 0 to 1000 mr/hr. In addition, two CDV 700-Model 6A "Geiger" meters were available for personnel monitoring or for low range survey measurements such as surveying the outer exclusion fence.

Two Nuclear Measurements Corporation Model BA-2A Radiation Alarms were used to monitor the radiation level at the test facility. A low range Model BA-2A, 0-50 mr unit monitors dose level within the control building while a high range 0-10,000 mr unit connected to a recorder monitors and records the dose level in the test field. Activation of either of these alarms above preset levels causes a warning bell to ring and a red light to come on. All personnel entering the test site wear both film badges and 200 mr CDV 138 self reading dosimeters.

CHAPTER 3

EXPERIMENTAL TECHNIQUES AND INSTRUMENT CALIBRATION

3.1 General

This chapter summarizes the techniques used in the calibration of test sources and instruments and the procedures used in the performance of the experiments. A total of three different sources of activity and instruments with three different ranges were used in the collection of the data. Each of these instruments and sources had to be calibrated not only with respect to each other but also on an absolute basis.

3.2 Calibration of the Test Instrumentation

Data was obtained using Victoreen Model 362, 239, and 208 non-direct reading ionization chambers together with a Technical Operations Model 556 Reader-Charger. These dosimeters and their associated reading instrumentation were tested to determine (a) variations among dosimeters when subject to the same amount of radiation exposure, and (b) constants and equations that can be used to obtain corrected radiation dose values. To group the detectors according to response characteristics, sets of ionization chambers (of a single type) were positioned at a constant distance from a source of known strength and exposed for a fixed period of time. The sets generally consisted of 35 to 75 dosimeters which were mounted vertically and in a circle around the test source. At the center of the circle a 0.55 curie cobalt-60 source was exposed at the same height as the detectors. The parameters of detector height, exposure time, etc. used for each detector are presented in Table 3.1.

All dosimeters were subjected to at least three exposures of equal time and an average of the three exposures was obtained for each dosimeter. The exposure level was indicated by a Technical Operations Model 556 Charger-Reader which gives readings in arbitrary units labeled microamperes. These readings may be converted to milliroentgens by use of experimentally determined constants. For the purpose of grouping dosimeters into lots of similar responses, however, the microampere (μa) values were

TABLE 3.1

DOSIMETER COMPARISON CHARACTERISTICS

Model	Nominal Range (mr)	Source to Detector Distance (ft.)	Height (ft.)	Exposure Time (min.)
362	0-200	3	2.5	8.0
239	0-10	20	3.	15.0
208	0-1	52	2.5	15.0

sufficient. These ua values were standardized by correcting for atmospheric pressure and temperature. Additionally, in each exposure, two Victoreen Model 130 ionization chambers (calibrated by the Bureau of Standards) were positioned with the dosimeters and used to check the dose uniformity.

On the basis of these tests it was found that the Model 239 chambers grouped within $\pm$ 1.7% of the mean value and the Model 208 chambers grouped within $\pm$ 3% of the mean value. The Model 362 chambers, however, showed considerable spread and were regrouped into lots containing dosimeters that gave a response of $\pm$ 2% to a given gamma ray dose. From the complete batch of 500 of the Model 362 dosimeters, 475 of them were divided into four groupings, and each group was identified by a color code. Twenty five Model 362 dosimeters could not be included in these groups as their exposure responses were outside the range listed. These were not used in the experiments.

Since the response of a dosimeter is indicated in microamperes when using the Technical Operations Model 556 Charger-Reader, it was necessary to develop a relationship between the Charger-Reader reading and the radiation dose. From this relationship calibration constants can be established for each of the three dosimeter types.

First, it was required to establish whether or not the dosimeter Charger-Reader combination had linear characteristics with respect to radiation dose. A series of calibration runs were made for each type of dosimeter using the 0.55 curie source. Both

the source and dosimeters were mounted eight feet from the ground. Exposures were made at source to detector distances of four to fifty feet with exposure times varying from one to twenty-four minutes.

The dose present at each of the various dosimeter positions was calculated from the relationship:

$$D_o = \frac{S_o \, t \, (14,000) e^{-\mu x} B(\mu x) \quad B(h, x)}{x^2} \qquad 3.2.1$$

where D_o = Dose in milliroentgens

S_o = Source strength in curies

14,000 = Dose rate one foot from one curie of Co-60 mr/hr

μ = Total air cross section at standard conditions = 1/448

h = Source and detector height

x = Source to detector distance in feet

$B(h, x)$ = Ground buildup factor (Reference 11)

t = Time in hours

$B(\mu x)$ = Air buildup factor for infinite media

The data from each exposure was then corrected for temperature and pressure and plotted to give a curve of dosimeter readings versus the calculated dose. This calibration curve is linear to about 60 microamperes and deviates slightly from linearity above this point. From this data and the known characteristics of the chambers an expression to convert the Charger-Reader readings to milliroentgens may be developed. If the relationship were linear over the entire range of exposures the following expression would be employed.

$$mr = k\left(\frac{P_1 T_2}{T_1 P_2}\right) \quad \mu_a \qquad 3.2.2$$

where k = The slope of the μ_a - mr graph

P_1 = Atmospheric pressure, inches Hg, on the day of calibration

T_1 = Absolute temperature degrees Rankine on the day of calibration

P_2 = Atmospheric pressure, inches Hg, at time of running any experiment

T_2 = Absolute temperature, degrees Rankine, at time of running any experiment

μ_a = Reading of Charger-Reader in microamperes

For convenience the values of k_1, P_1, T_1, can be combined into a constant C giving

$$mr = \left(\frac{T_2}{P_2 C}\right) \mu_a \qquad 3.2.3$$

To account for the deviation from a straight line a value x is introduced into the equation giving

$$mr = \frac{T}{PC} \quad (\mu_a + x) \qquad 3.2.4$$

Note that the subscripts for T and P were eliminated since these are now the only temperature and pressure terms in the equation. The values of x and C for the three types of dosimeters are presented in Table 3.2.

TABLE 3.2

CALIBRATION CONSTANTS FOR VICTOREEN CHAMBERS USING THE T/O MODEL 556 CHARGER-READER

$$\text{Measured dose (mr)} = \frac{T}{CP} \quad (\mu_a + x)$$

where

T = Temperature-degrees Fahrenheit absolute

P = Atmospheric pressure-inches of Hg

μ_a = Microamp reading

C = Calibration constant

x = Corrections for non-linearity at high values of μ_a

Dosimeter Type	"C"	Value x for μ_a readings of						
		0-64	65-69	70-74	75-79	80-84	85-89	90-95
Model 362								
"Brown" group	7.85	0.0	0.5	1.0	1.5	2.0	3.0	---
"Orange" group	8.03	0.0	0.5	1.0	1.5	2.0	3.0	---
"Blue" group	8.48	0.0	0.5	1.0	1.5	2.0	3.0	---
"Red and Green" group	8.54	0.0	0.5	1.0	1.5	2.0	3.0	---
Model 239	206	0.0	0.5	1.0	2.0	2.5	--	---
Model 208	1150	0.0	0.0	0.0	0.0	0.0	1.0	---

Comparison experiments were continually performed on the two Charger-Reader instruments throughout the experimental program. No detectable difference in readings was observed for the dosimeters exposed to identical dose values. It was determined that dosimeters could be charged with one Reader-Charger and read on the second Reader-Charger with no observable differences. In all experiments a Bureau of Standards calibrated Victoreen R-meter was employed as a base measurement and as a check on calculated methods.

3.3 Source Calibration

Three sources of cobalt-60 were required to conduct the open field and steel skeleton tests. These sources were of approximately 6, 60, and 600 curies strength. The active portion of each of these sources was of cylindrical shape 5/16 inches in diameter and approximately one inch long. Each of these sources was calibrated by determining its roentgen equivalent output with the source positioned side on (in a radial direction) with two standard ionization chambers. Calibration measurements were made for two source and detector arrangements, first, with the source on the ground (a concrete surface) and the detector in the air, and, secondly, with both source and detector at the same height above a concrete pad.

Roentgen output of the sources was determined using two Victoreen

Model 552 (2.5R) or two Model 130 (0.25R) chambers. These chambers were charged and read on a Victoreen Model 570 R-meter. The chambers together with the Charger-Reader were calibrated by the National Bureau of Standards on December 19, 1963. This calibration showed that the readings at standard atmospheric conditions taken with the Model 552 and 130 chambers must be multiplied by 0.95 and 1.04 respectively to obtain correct readings. Temperature and pressure correction factors at other than standard conditions are:

Model 552 = 0.0537 T/P

Model 130 = 0.0585 T/P

Where T = temperature in degrees Rankine absolute
P = pressure at the time of calibration in inches Hg

Reproducibility with both instruments was better than $\pm$ 1 percent at midscale. The source strength for the two source and detector arrangements was then determined from the equations:

Source on the ground, detector in the air

$$D_o = \frac{q_o S_o e^{-\mu\rho} B_1(\mu\rho)}{\rho^2} \qquad 3.3.1$$

Source and detector suspended in air

$$D_o = \frac{q_o S_o e^{-\mu d} B_2(\mu d) B_3(h, d)}{d^2} \qquad 3.3.2$$

where

D_o = measured dose rate - R/hour
q_o = specific irradiance R/hour at 1 ft. distance
S_o = source strength in curies
μ = total cross section for cobalt-60 radiation ($1/448$ ft^{-1})

ρ - slant distance source to detector (ft.)

h = height of the source and detector (ft.)

d = horizontal source to detector distance (ft.)

$B_1(\mu\rho)$ - air and ground buildup factor for source on the ground detector in the air (see Ref. 9)

$B_2(\mu, d)$ calculated air buildup factor (see Ref. 10)

$B_3(h, d)$ ground scatter coefficient (see Ref. 11)

The maximum difference of the source strengths as determined from each geometric arrangement and the appropriate equation was less than 1.3 percent. The actual equivalent source strength as measured corrected for time decay to March 1, 1964 are.

Source No. 1	539 curies
Source No. 2	52.8 curies
Source No. 3	5.28 curies

3.4 Operating Procedures

All personnel entering the Radiation Test Facility are required to carry both 200 mr direct reading dosimeters and film badges. At the beginning of an experiment test exposure dosimeters are charged and placed in various positions within or around the test structure. All persons within the exclusion area are then accounted for and preparations are begun for an actual exposure. The appropriate source container is positioned in its proper location, and prior to unlocking this container the outer fence warning lights are turned on and a check made to insure that the area monitoring devices are operating properly.

The detailed operational procedures followed in the use of the Conesco Model F-12% Hydraulic Source Circulation System are presented in step-by-step fashion as follows. (Reference is made to the schematic diagram of Figure 2.6)

(1) Select the proper pumps and pump operating speeds by presetting the pump strokes, valves and switches on the pumping console.

(2) Connect the pumping console directly to the source travel tubing. Insert an empty source assembly (dummy) into the inlet line of

the source travel t ing.

(3) Turn on pumps, tu on solenoid valve (key lock switch), and observe travel of dummy source through the tubing.

(4) Upon completion of steps 1 through 3, close solenoid valve, remove dummy source from tubing, shut off all pumps.

Note. Steps 1 through 4 ensure that the tubing has not been damaged. Steps 5 through 18 should be performed by a team of two operators – one to perform the operations, the other to monitor the performance; each operator should have a radiation survey meter.

(5) Select either the 6, 60 or 600 curie source to be used. Be certain that source is clamped, remove shipping plugs. Inspect the source piston leather and replace it if necessary.

(6) Connect tubing from the field to source storage container and from the storage container to the return line of the pump console.

(7) Connect pressure lead from pumps to rear of source assembly.

(8) Unclamp source assembly.

(9) Select and preset pumps to desired pumping speed by setting valves on pumping console. Start pumps.

(10) Retire to control bunker and operate solenoid valve (key lock switch).

(11) Wait until exposure is complete and source has returned to storage container.

(12) Return solenoid valve (key lock switch) to OFF position (pilot light on).

(13) Turn off all pumps.

(14) Approach storage container using hand-held survey meters, and clamp source by tightening source clamp.

(15) Disconnect pressure tube from source storage container; allow 5 minutes for pressure to bleed down.

(16) Disconnect all remaining tubes from the storage container and insert shipping plugs.

(17) Replace padlocks on shipping plugs.

(18) Return to Step 1 for next run, or step 5 for a re-run.

3.5 Normalization of Data

All dosimeter readings obtained were normalized to a "per hour basis" for an equivalent contamination density of one curie per square foot*. Because of the large number of dosimeter readings to be taken in the test series, data normalization was programmed for the RCA 301 computing machine. In this program dosimeter readings are converted to an mr/hr basis using dosimeter calibration constants, the exposure time, source strength, and the atmospheric temperature-pressure corrections covered in Section 3.2 of this report. The equation used to correct readings of milliroentgens to a standard curie per square foot basis is;

$$I_o = \frac{DA}{T' S_o} \qquad 3.5.1$$

where

I_o = the normalized data in (R/hr)/(curie/ft.^{2})

D = the measured dose rates normalized to standard conditions of pressure and temperature

A = area of the contaminated field (ft.^{2})

S_o = source strength (curies)

T' = exposure time (hours)

* This source density of cobalt-60 produces a radiation field of 464 R/hr at a 3-ft height above an infinite smooth uniformly contaminated plane

CHAPTER IV

DESCRIPTION OF EXPERIMENTAL DATA

4.1 GENERAL

This report covers two series of experiments. The first series was devoted to determining the dose rate above an open field so that it could be used as a standard reference in the interpretation of later test results obtained on actual structures. The second series was to evaluate the effects introduced by the permanent steel frame used to support the concrete slabs of the various test structures. Each of these series of experiments were performed in the same way so that direct comparisons of results could be made.

Unfortunately it was not possible to remove the steel frame for the conducting of the open field tests and, as was discussed in Chapter 2, the experimental set-up was shifted 75 feet to one side of the steel frame for these tests (See Figure 2.5). Other than this position change the open field experiments were ser up and performed in the same way as those on the steel structure.

4.2 REPRODUCIBILITY OF EXPERIMENTAL DATA

Since an experiment of this type requires many separate runs to obtain a complete set of data it is important to determine the accuracy to which the data may be reproduced. To determine this accuracy a set of twenty "identical" experiments were conducted with variations in the parameters of source size, temperature, atmospheric pressure, and exposure time. The standard deviation of the data was determined from these results. These experiments were conducted during a thirty day period in the spring of the year when atmospheric conditions were rapidly changing. The center three and nine foot height detector positions within the steel frame were used. Source exposure was made in Area 1. The variation of experimental parameters that occurred during this series of tests were;

Temperature	34.5 - 70° F
Atmospheric pressure	29.34 - 30.05 in. Hg.
Exposure time	2.9 - 42.8 minutes

Source strength	5.18 - 52.4 curies
Weather	cloudy to clear
	still to high gusts

The data obtained from these experiments was normalized in the standard manner (see Chapter 3) and is presented in Figure 4.1. The standard deviation is 2.2 and 2.4 percent for the data obtained at three and nine foot heights respectively. Though the total number of twenty experiments is small enough so that there may be a little doubt as to the accuracy of this standard deviation, the data obtained from the open field and other experiments probably does not differ significantly from the value obtained.

4.3 OPEN FIELD TESTS

To determine the contribution from the test field in the absence of any structure, test runs were made with the quarter field tubing symmetry described in Chapter 2 (see Figure 2.5). As it was not possible to remove the steel frame the tubing field was offset from the steel frame by approximately seventy-five feet to obtain an unobstructed area.

Detector positions similar to those established for experiments with the test structure were laid out to create a "phantom" arrangement at the apex of the field. A plan view of this array of standard positions is shown in Figure 4.2. The standard arrangement of dosimeter positions consisted of a grid of vertical arrays along the width at five selected dimensions, and five vertical arrays along the length at five selected positions for a total of twenty-five vertical arrays. The area occupied by dosimeters is 44 feet long and 32 feet wide. These dimensions were selected to accommodate a duplicate dosimeter arrangement for use with the steel frame structure. The outermost standard positions will thus fall outside the building while the remaining dosimeters will be inside the structure.

Each dosimeter of the vertical array was supported and held in position by being tied to a vertical string. The vertical strings in turn were held in place by a system of tall poles and rope rigging of minimum mass.

The instruments used were two Victoreen Model 362, 200 mr Chamber Dosimeters (at each position) at elevations of 1, 3, 6, 9, 15, 21, 24, 27, and 30 feet, and

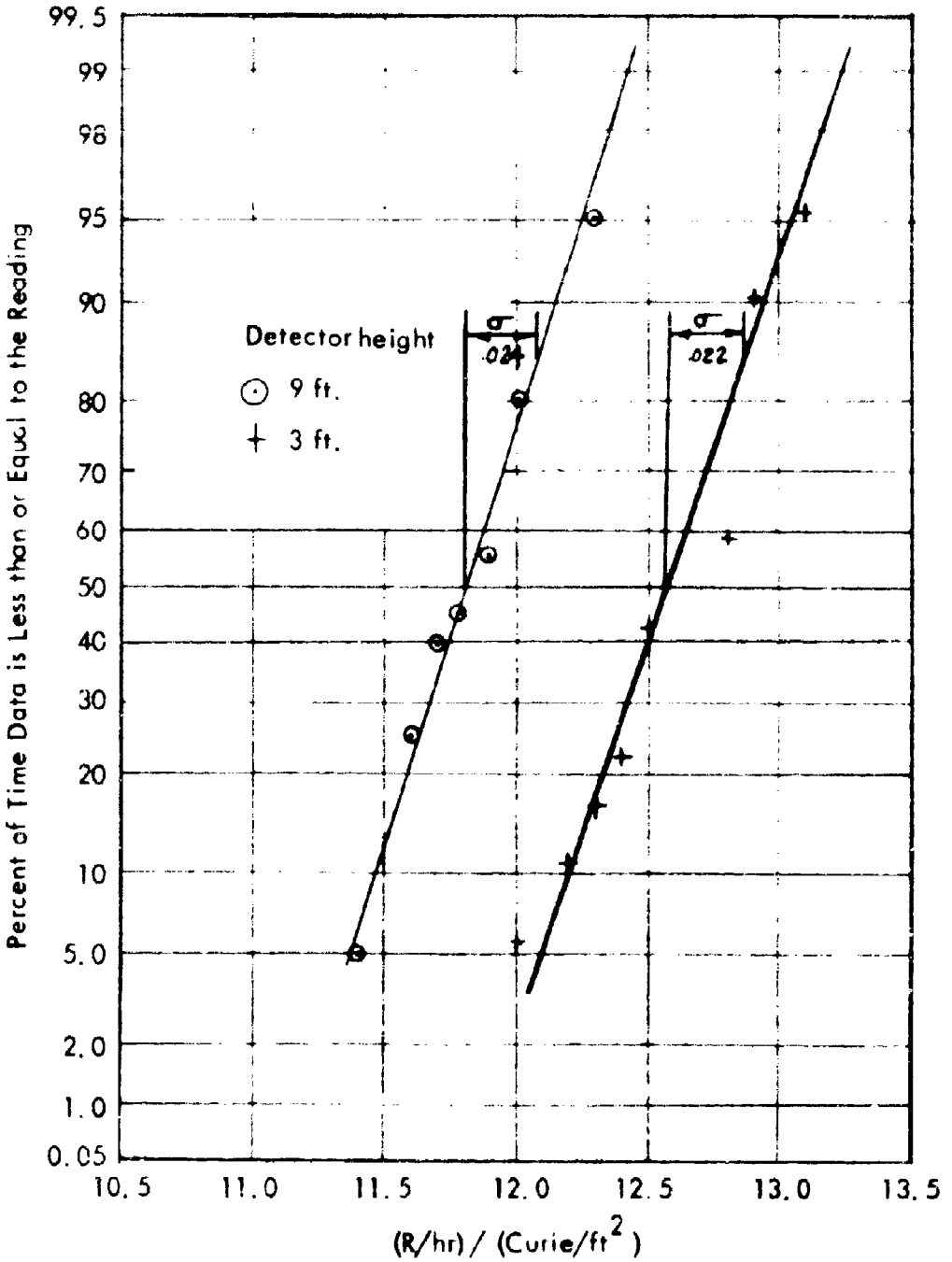

Figure 4.1 - Statistical Analysis of Data

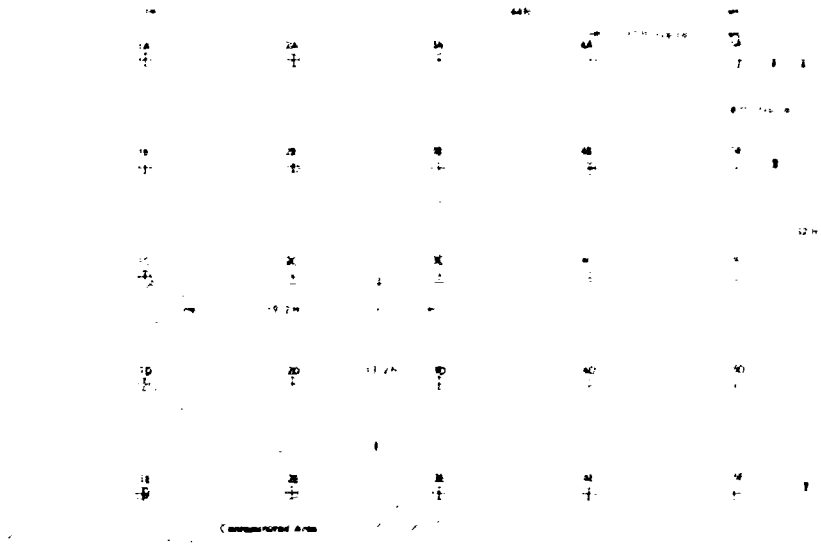

Figure 4.2 - Plan View of Dosimeter Locations for the Open Field Test

a single dosimeter at 33 feet height. The center array, however, also contained two dosimeters at the 33 foot height. Dual dosimeter positions and replications of test runs were used as a data check. The data obtained from this series of tests has been normalized to a uniform source density (one curie/ft.^{2}) and is presented in Tables 4.1, 4.2, 4.3, 4.4, and 4.5. Since there was purposeful duplications both in test runs and detectors during this series of experiments the values shown in the tables are the median values of the test results obtained.

TABLE 4.1
OPEN FIELD EXPERIMENTAL VALUES
AREA 0 (R/hr)/(Curie/ft.^{2})

Height (ft.)	Dose Rate Quarter Field	Dose Rate Full Field
1	56.41	225.64
3	39.86	159.44
6	26.48	105.92
9	18.44	73.76
15	10.19	40.76
18	7.91	31.64
21	6.39	25.56
27	3.76	15.04
30	3.21	12.88
33	2.70	10.80

TABLE 4.2

DOSE RATE IN AIR FIELD

(r/hr normalized to source density of 1 curie/ft²)

AREA 1A

POSITION	HEIGHT 1	3	6	9	ABOVE 15	18	GROUND 21	27	30	33
1 A	7.10	6.48	[illegible]	7.37	6.52	[illegible]	[illegible]	[illegible]	[illegible]	[illegible]
B	17.99	17.64	16.41	15.10	9.64	[illegible]	[illegible]	[illegible]	[illegible]	[illegible]
C	90.64	60.41	36.40	26.74	15.50	11.76	[illegible]	[illegible]	[illegible]	[illegible]
D	200.66	100.90	60.41	[illegible]	19.34	15.63	11.46	[illegible]	[illegible]	[illegible]
E	200.56	113.66	[illegible]	[illegible]	19.53	[illegible]	[illegible]	[illegible]	[illegible]	[illegible]
2 A	6.69	7.62	[illegible]	[illegible]	[illegible]	[illegible]	[illegible]	[illegible]	[illegible]	[illegible]
B	11.63	12.67	[illegible]	[illegible]	[illegible]	[illegible]	[illegible]	[illegible]	[illegible]	[illegible]
C	22.03	23.16	[illegible]	[illegible]	[illegible]	[illegible]	[illegible]	[illegible]	[illegible]	[illegible]
D	[illegible]	[illegible]	[illegible]	[illegible]	[illegible]	[illegible]	[illegible]	[illegible]	[illegible]	[illegible]
E	[illegible]	[illegible]	[illegible]	[illegible]	[illegible]	[illegible]	[illegible]	[illegible]	[illegible]	[illegible]
3 A	[illegible]	[illegible]	[illegible]	[illegible]	[illegible]	[illegible]	[illegible]	[illegible]	[illegible]	[illegible]
B	[illegible]	[illegible]	[illegible]	[illegible]	[illegible]	[illegible]	[illegible]	[illegible]	[illegible]	[illegible]
C	[illegible]	[illegible]	[illegible]	[illegible]	[illegible]	[illegible]	[illegible]	[illegible]	[illegible]	[illegible]
D	[illegible]	[illegible]	[illegible]	[illegible]	[illegible]	[illegible]	[illegible]	[illegible]	[illegible]	[illegible]
E	[illegible]	[illegible]	[illegible]	[illegible]	[illegible]	[illegible]	[illegible]	[illegible]	[illegible]	[illegible]
4 A	[illegible]	[illegible]	[illegible]	[illegible]	[illegible]	[illegible]	[illegible]	[illegible]	[illegible]	[illegible]
B	[illegible]	[illegible]	[illegible]	[illegible]	[illegible]	[illegible]	[illegible]	[illegible]	[illegible]	[illegible]
C	[illegible]	[illegible]	[illegible]	[illegible]	[illegible]	[illegible]	[illegible]	[illegible]	[illegible]	[illegible]
D	[illegible]	[illegible]	[illegible]	[illegible]	[illegible]	[illegible]	[illegible]	[illegible]	[illegible]	[illegible]
E	[illegible]	[illegible]	[illegible]	[illegible]	[illegible]	[illegible]	[illegible]	[illegible]	[illegible]	[illegible]
5 A	[illegible]	[illegible]	[illegible]	[illegible]	[illegible]	[illegible]	[illegible]	[illegible]	[illegible]	[illegible]
B	[illegible]	[illegible]	[illegible]	[illegible]	[illegible]	[illegible]	[illegible]	[illegible]	[illegible]	[illegible]
C	[illegible]	[illegible]	[illegible]	[illegible]	[illegible]	[illegible]	[illegible]	[illegible]	[illegible]	[illegible]
D	[illegible]	[illegible]	[illegible]	[illegible]	[illegible]	[illegible]	[illegible]	[illegible]	[illegible]	[illegible]
E	[illegible]	[illegible]	[illegible]	[illegible]	[illegible]	[illegible]	[illegible]	[illegible]	[illegible]	[illegible]

POSITION										
1	A	[illegible]	[illegible]	[illegible]	[illegible]	[illegible]	[illegible]	[illegible]	[illegible]	[illegible]	[illegible]
	B	[illegible]	23.21	[illegible]	[illegible]	[illegible]	[illegible]	[illegible]	[illegible]	[illegible]	[illegible]
	C	[illegible]	[illegible]	[illegible]	[illegible]	[illegible]	[illegible]	[illegible]	[illegible]	[illegible]	[illegible]
	D	[illegible]	[illegible]	[illegible]	[illegible]	[illegible]	[illegible]	[illegible]	[illegible]	[illegible]	[illegible]
	E	[illegible]	[illegible]	[illegible]	[illegible]	[illegible]	[illegible]	[illegible]	[illegible]	[illegible]	[illegible]
2	A	[illegible]	[illegible]	[illegible]	[illegible]	[illegible]	[illegible]	[illegible]	[illegible]	[illegible]	[illegible]
	B	[illegible]	[illegible]	[illegible]	[illegible]	[illegible]	[illegible]	[illegible]	[illegible]	[illegible]	[illegible]
	C	[illegible]	[illegible]	[illegible]	[illegible]	[illegible]	[illegible]	[illegible]	[illegible]	[illegible]	[illegible]
	D	[illegible]	[illegible]	[illegible]	[illegible]	[illegible]	[illegible]	[illegible]	[illegible]	[illegible]	[illegible]
	E	[illegible]	[illegible]	[illegible]	[illegible]	[illegible]	[illegible]	[illegible]	[illegible]	[illegible]	[illegible]
3	A	[illegible]	[illegible]	[illegible]	[illegible]	[illegible]	[illegible]	[illegible]	[illegible]	[illegible]	[illegible]
	B	[illegible]	[illegible]	[illegible]	[illegible]	[illegible]	[illegible]	[illegible]	[illegible]	[illegible]	[illegible]
	C	[illegible]	[illegible]	[illegible]	[illegible]	[illegible]	[illegible]	[illegible]	[illegible]	[illegible]	[illegible]
	D	[illegible]	[illegible]	[illegible]	[illegible]	[illegible]	[illegible]	[illegible]	[illegible]	[illegible]	[illegible]
	E	[illegible]	[illegible]	[illegible]	[illegible]	[illegible]	[illegible]	[illegible]	[illegible]	[illegible]	[illegible]
4	A	[illegible]	[illegible]	[illegible]	[illegible]	[illegible]	[illegible]	[illegible]	[illegible]	[illegible]	[illegible]
	B	[illegible]	[illegible]	[illegible]	[illegible]	[illegible]	[illegible]	[illegible]	[illegible]	[illegible]	[illegible]
	C	[illegible]	[illegible]	[illegible]	[illegible]	[illegible]	[illegible]	[illegible]	[illegible]	[illegible]	[illegible]
	D	[illegible]	[illegible]	[illegible]	[illegible]	[illegible]	[illegible]	[illegible]	[illegible]	[illegible]	[illegible]
	E	[illegible]	[illegible]	[illegible]	[illegible]	[illegible]	[illegible]	[illegible]	[illegible]	[illegible]	[illegible]
5	A	[illegible]	[illegible]	[illegible]	[illegible]	[illegible]	[illegible]	[illegible]	[illegible]	[illegible]	[illegible]
	B	[illegible]	[illegible]	[illegible]	[illegible]	[illegible]	[illegible]	[illegible]	[illegible]	[illegible]	[illegible]
	C	[illegible]	[illegible]	[illegible]	[illegible]	[illegible]	[illegible]	[illegible]	[illegible]	[illegible]	[illegible]
	D	[illegible]	[illegible]	[illegible]	[illegible]	[illegible]	[illegible]	[illegible]	[illegible]	[illegible]	[illegible]
	E	[illegible]	[illegible]	[illegible]	[illegible]	[illegible]	[illegible]	[illegible]	[illegible]	[illegible]	[illegible]

A										
B										
C										
D										
E										
A										
B										
C										
D										
E										
A										
B										
C										
D										
E										
A										
B										
C										
D										
E										

4.4 CALIBRATION OF THE STEEL STRUCTURE

Following the open field "calibration", the second of the basic calibrations was made, that of determining the effect of the bare steel frame on the radiation field. A quarter symmetry field identical to that used in the open field calibration was employed. This field was laid out with the center of the structure coinciding with the apex point of the field. Since this field was only slightly offset from the open field test, the physical features of the actual ground, as to roughness and ground surface material, were very nearly identical.

The same arrangement of detector positions was used for these experiments as for the open field tests. (The same methods of dosimeter support was also used). The plan locations of each position are shown in the sketch Figure 4.3. The outside

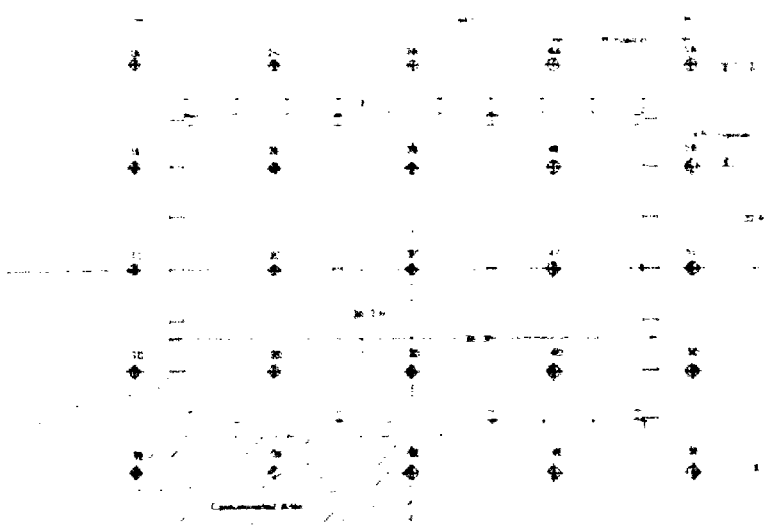

Figure 4.3 - Plan View of Dosimeter Locations for the Skeleton Test

perimeter of the dosimeter arrays used in the calibration of the steel test structure, a total of sixteen array locations, fall outside the structure by a distance of three and a half feet. The remaining nine dosimeter array locations are within the structure. Two dosimeters were located at each position in an array at heights of 1, 3, 6, 7, 15, 18, 21, 27, and 30 feet, and a single dosimeter was placed at 33 feet.

The data obtained from this series of experiments is presented in Tables 4.6, 4.7, 4.8, and 4.9 for each experimental area and each detector location. As in the open field tests many duplicate readings were obtained from test replications and doubling up of test instruments. The median results are presented in these tables. The data is normalized to a contamination density of one curie per square foot.

4.5 DOSE VARIATION WITHIN THE STRUCTURE

It is of interest to examine dose variation as a function of position within the steel structure. From theoretical considerations the dose variation within the steel skeleton should be similar to the variation in the open field tests except in regions where it is modified by the attenuation effects of the structure. Figures 4.4 through 4.7 show several typical horizontal and vertical plots of dose rate versus position within the steel structure and in the open field. The data is for a full field of contamination extending to a radius of 452 feet and surrounding the structure on all sides (a quarter field was actually run and symmetrical dosimeter readings were added). Inspection of these figures shows that the dose rate contour shapes for the steel frame and the open field are similar except in the vicinity of the steel beams of the structure where the contour shapes are different.

TABLE 4.6

DOSE RATE IN [illegible]

(r/hr normalised to source density of 1 curie/ft^2)

POSITION	HEIGHT ABOVE GROUND (ft)									
	1	3	6	9	15	18	21	27	30	33
1 A	6.28	7.03	7.19	7.19	7.19	5.51	3.00	3.45	3.44	3.42
B	16.12	16.21	16.12	13.81	9.[illegible]	7.26	5.[illegible]9	4.36	3.[illegible]	3.56
C	112.16	66.61	39.77	25.59	14.51	10.[illegible]	8.[illegible]	6.12	5.57	4.29
D	192.91	114.78	55.99	35.13	16.93	13.[illegible]	10.[illegible]	6.91	5.15	4.[illegible]
E	213.11	121.13	66.62	43.91	21.50	17.43	13.76	9.03	7.65	6.05
2 A	4.[illegible]	5.[illegible]	5.[illegible]	5.31	3.[illegible]	3.02	2.[illegible]	2.[illegible]	2.[illegible]	1.[illegible]
B	[illegible]	[illegible]	[illegible]	[illegible]	6.6[illegible]	5.[illegible]	4.[illegible]	3.[illegible]	3.[illegible]	2.[illegible]
C	[illegible]	[illegible]	[illegible]	[illegible]	[illegible]	[illegible]	7.31	[illegible]	[illegible]	3.[illegible]
D	44.15	43.60	36.51	25.[illegible]	14.[illegible]	12.[illegible]	10.04	6.[illegible]	5.[illegible]	4.[illegible]
E	232.74	126.52	67.59	43.60	21.26	16.01	12.63	7.90	6.36	5.[illegible]
3 A	3.70	4.11	4.37	4.23	2.39	2.67	2.[illegible]	1.84	1.50	1.53
B	7.30	7.66	7.91	7.90	4.05	4.23	3.86	2.76	2.62	2.39
C	12.16	12.89	12.48	11.92	5.89	5.78	5.57	3.55	3.28	3.00
D	22.62	23.24	19.46	15.57	9.39	8.42	7.15	4.91	3.49	3.[illegible]
E	122.69	70.90	42.51	28.70	15.[illegible]	12.56	10.58	7.28	5.95	5.46
4 A	2.31	2.94	2.99	2.94	1.72	1.77	1.69	1.16	1.00	1.04
B	3.[illegible]	4.54	4.63	4.[illegible]	2.[illegible]	2.59	2.59	1.78	1.[illegible]	1.70
C	4.97	5.53	5.[illegible]	5.[illegible]	3.15	3.33	3.17	2.30	2.24	2.07
D	6.66	7.56	7.22	6.77	4.17	4.[illegible]	4.20	2.53	2.47	2.42
E	11.23	12.65	11.73	11.70	8.[illegible]	7.23	6.[illegible]	4.[illegible]	4.17	3.92
5 A	1.35	1.66	1.73	1.73	1.11	1.11	1.11	0.67	0.70	0.99
B	2.18	2.[illegible]	2.[illegible]	2.[illegible]	1.[illegible]	1.[illegible]	1.[illegible]	1.23	1.39	1.20
C	2.62	3.06	3.17	3.11	2.04	2.07	1.90	1.[illegible]	1.49	1.40
D	3.22	3.79	3.73	3.73	2.57	2.57	2.60	1.[illegible]	1.73	1.61
E	3.44	4.[illegible]	4.55	4.55	4.56	4.39	3.92	3.[illegible]	3.04	2.79

TABLE 4.7

DOSE RATE IN SKELETON STRUCTURE

[illegible] normalized to source density of 1 curie/ft^2

AREA 2 (QUARTER SYMMETRY)

			BELOW		ABOVE		GROUND		(Ft)	
[illegible]	1	5	6	10	15	20	21	25	30	35
1 A	24.25	24.46	23.83	23.83	24.34	23.50	23.07	22.03	21.59	21.09
B	28.95	29.87	29.04	28.30	27.59	26.42	27.23	25.53	24.05	23.07
C	36.05	36.53	35.28	34.01	34.01	34.01	32.36	28.85	27.37	25.71
D	53.11	53.11	50.40	43.42	38.59	38.56	37.52	33.26	31.07	29.45
E	79.37	78.24	72.11	65.13	46.91	41.09	38.34	37.14	34.81	31.82
2 A	7.32	10.12	9.37	10.04	8.35	8.42	8.10	8.34	8.10	8.14
B	13.45	13.58	14.07	14.68	13.15	12.48	12.48	9.55	9.55	9.55
C	17.62	19.09	19.16	18.72	12.85	14.87	14.31	12.24	11.26	11.26
D	30.03	30.80	29.26	25.10	21.56	19.49	18.72	13.99	14.69	14.69
E	44.65	43.85	43.85	40.80	33.87	30.10	26.95	17.98	15.78	15.23
3 A	6.93	7.72	8.24	8.24	4.84	6.27	6.41	4.84	4.84	4.51
B	10.35	11.30	11.33	11.33	8.90	9.87	9.86	6.98	7.15	6.16
C	14.42	14.42	15.62	15.62	9.53	11.79	11.83	8.15	8.62	8.62
D	17.00	17.71	16.11	17.37	15.34	15.15	14.05	10.35	11.09	10.60
E	28.69	28.69	27.91	25.97	20.70	20.36	19.97	16.77	15.57	14.37
4 A	5.21	5.35	6.28	6.35	3.65	3.72	4.60	3.65	3.65	3.45
B	7.39	8.67	8.16	8.79	5.28	5.66	7.03	5.66	5.55	5.44
C	9.92	9.94	10.20	10.71	7.14	8.16	8.16	6.63	6.09	6.63
D	11.22	12.23	12.23	11.98	10.45	10.96	10.20	8.92	8.66	8.67
E	16.44	15.75	15.35	17.97	15.48	15.29	15.10	12.61	11.73	11.73
5 A	3.25	3.90	4.16	4.35	2.47	2.47	2.99	2.72	2.60	2.60
B	4.68	5.65	6.24	5.91	3.52	4.35	4.61	3.64	3.70	3.70
C	5.55	6.43	6.63	6.49	4.87	5.68	5.41	4.46	4.33	4.46
D	5.02	7.63	7.35	8.54	6.62	6.49	6.37	5.46	5.26	5.33
E	10.32	10.70	11.99	11.51	11.01	11.01	10.40	10.40	9.06	8.81

AREA 3

			HEIGHT		ABOVE		GROUND	(FT)		
[illegible]	[illegible]	[illegible]	[illegible]	[illegible]	[illegible]	[illegible]	[illegible]	[illegible]	[illegible]	[illegible]
A	[illegible]	[illegible]	[illegible]	[illegible]	[illegible]	[illegible]	[illegible]	[illegible]	[illegible]	[illegible]
B	[illegible]	[illegible]	21.36	22.03	[illegible]	22.23	21.82	21.82	21.82	21.23
C	[illegible]	[illegible]	[illegible]	[illegible]	[illegible]	[illegible]	[illegible]	23.77	23.00	22.04
D	[illegible]	[illegible]	[illegible]	[illegible]	[illegible]	[illegible]	[illegible]	[illegible]	[illegible]	[illegible]
E	[illegible]	[illegible]	[illegible]	[illegible]	33.72	[illegible]	33.07	32.03	32.31	32.07
A	[illegible]	[illegible]	[illegible]	[illegible]	[illegible]	[illegible]	[illegible]	[illegible]	[illegible]	[illegible]
B	[illegible]	[illegible]	[illegible]	[illegible]	[illegible]	[illegible]	[illegible]	[illegible]	16.02	16.31
C	[illegible]	[illegible]	[illegible]	[illegible]	[illegible]	[illegible]	[illegible]	[illegible]	[illegible]	[illegible]
D	[illegible]	[illegible]	[illegible]	[illegible]	[illegible]	[illegible]	[illegible]	[illegible]	[illegible]	[illegible]
E	[illegible]	[illegible]	[illegible]	[illegible]	[illegible]	[illegible]	[illegible]	[illegible]	[illegible]	[illegible]
A	[illegible]	[illegible]	[illegible]	[illegible]	[illegible]	[illegible]	[illegible]	[illegible]	[illegible]	[illegible]
B	[illegible]	[illegible]	[illegible]	[illegible]	[illegible]	[illegible]	[illegible]	[illegible]	[illegible]	[illegible]
C	[illegible]	[illegible]	[illegible]	[illegible]	[illegible]	[illegible]	[illegible]	[illegible]	[illegible]	[illegible]
D	[illegible]	[illegible]	[illegible]	[illegible]	[illegible]	[illegible]	[illegible]	[illegible]	[illegible]	[illegible]
E	[illegible]	[illegible]	[illegible]	[illegible]	[illegible]	[illegible]	[illegible]	[illegible]	[illegible]	[illegible]
A	[illegible]	[illegible]	[illegible]	[illegible]	[illegible]	[illegible]	[illegible]	[illegible]	[illegible]	[illegible]
B	[illegible]	[illegible]	[illegible]	[illegible]	[illegible]	[illegible]	[illegible]	[illegible]	[illegible]	[illegible]
C	[illegible]	[illegible]	[illegible]	[illegible]	[illegible]	[illegible]	[illegible]	[illegible]	[illegible]	[illegible]
D	[illegible]	[illegible]	[illegible]	[illegible]	[illegible]	[illegible]	[illegible]	[illegible]	[illegible]	[illegible]
E	20.67	23.77	24.30	25.49	25.49	26.79	26.79	23.81	23.82	23.82
A	[illegible]	[illegible]	[illegible]	[illegible]	[illegible]	[illegible]	[illegible]	[illegible]	[illegible]	[illegible]
B	[illegible]	[illegible]	[illegible]	[illegible]	[illegible]	[illegible]	[illegible]	[illegible]	[illegible]	[illegible]
C	[illegible]	[illegible]	[illegible]	[illegible]	[illegible]	[illegible]	[illegible]	[illegible]	[illegible]	[illegible]
D	[illegible]	[illegible]	[illegible]	[illegible]	[illegible]	[illegible]	[illegible]	[illegible]	[illegible]	[illegible]
E	[illegible]	[illegible]	[illegible]	[illegible]	[illegible]	[illegible]	[illegible]	[illegible]	[illegible]	[illegible]
A	[illegible]	[illegible]	[illegible]	[illegible]	[illegible]	[illegible]	[illegible]	[illegible]	[illegible]	[illegible]
B	[illegible]	[illegible]	[illegible]	[illegible]	[illegible]	[illegible]	[illegible]	[illegible]	[illegible]	[illegible]
C	[illegible]	[illegible]	[illegible]	[illegible]	[illegible]	[illegible]	[illegible]	[illegible]	[illegible]	[illegible]
D	[illegible]	[illegible]	[illegible]	[illegible]	[illegible]	[illegible]	[illegible]	[illegible]	[illegible]	[illegible]
E	[illegible]	[illegible]	[illegible]	[illegible]	[illegible]	[illegible]	[illegible]	[illegible]	[illegible]	[illegible]

[illegible]	I	II	III	IV	V	VI	VII	VIII	IX	X
1 A	[illegible]	[illegible]	[illegible]	[illegible]	[illegible]	[illegible]	[illegible]	[illegible]	[illegible]	[illegible]
B	[illegible]	[illegible]	[illegible]	[illegible]	[illegible]	[illegible]	[illegible]	[illegible]	[illegible]	[illegible]
C	[illegible]	[illegible]	[illegible]	[illegible]	[illegible]	[illegible]	[illegible]	[illegible]	[illegible]	[illegible]
D	[illegible]	[illegible]	[illegible]	[illegible]	[illegible]	[illegible]	[illegible]	[illegible]	[illegible]	[illegible]
E	[illegible]	[illegible]	[illegible]	[illegible]	[illegible]	[illegible]	[illegible]	[illegible]	[illegible]	[illegible]
2 A	[illegible]	[illegible]	[illegible]	[illegible]	[illegible]	[illegible]	[illegible]	[illegible]	[illegible]	[illegible]
B	[illegible]	[illegible]	[illegible]	[illegible]	[illegible]	[illegible]	[illegible]	[illegible]	[illegible]	[illegible]
C	[illegible]	[illegible]	[illegible]	[illegible]	[illegible]	[illegible]	[illegible]	[illegible]	[illegible]	[illegible]
D	[illegible]	[illegible]	[illegible]	[illegible]	[illegible]	[illegible]	[illegible]	[illegible]	[illegible]	[illegible]
E	[illegible]	[illegible]	[illegible]	[illegible]	[illegible]	[illegible]	[illegible]	[illegible]	[illegible]	[illegible]
3 A	6.22	9.31	[illegible]	[illegible]	[illegible]	[illegible]	[illegible]	[illegible]	[illegible]	[illegible]
B	[illegible]	[illegible]	[illegible]	[illegible]	[illegible]	[illegible]	[illegible]	[illegible]	[illegible]	[illegible]
C	[illegible]	[illegible]	13.76	[illegible]	[illegible]	15.22	[illegible]	[illegible]	[illegible]	[illegible]
D	[illegible]	11.66	13.60	[illegible]	14.22	[illegible]	[illegible]	[illegible]	[illegible]	[illegible]
E	11.01	14.90	17.17	[illegible]	[illegible]	[illegible]	20.64	21.34	20.52	20.99
4 A	[illegible]	7.74	9.26	[illegible]	[illegible]	[illegible]	10.72	[illegible]	10.35	[illegible]
B	7.37	10.05	11.56	12.06	[illegible]	[illegible]	13.73	12.39	13.73	[illegible]
C	7.70	10.05	12.06	12.72	[illegible]	14.07	13.39	14.06	13.73	[illegible]
D	[illegible]	10.72	12.39	12.39	[illegible]	14.40	14.40	14.40	[illegible]	[illegible]
E	10.22	[illegible]	[illegible]	[illegible]	[illegible]	15.42	[illegible]	[illegible]	[illegible]	[illegible]
5 A	[illegible]	[illegible]	7.27	[illegible]	[illegible]	[illegible]	[illegible]	[illegible]	[illegible]	[illegible]
B	[illegible]	7.60	[illegible]	[illegible]	10.61	10.34	10.59	[illegible]	[illegible]	[illegible]
C	[illegible]	[illegible]	9.60	[illegible]	10.72	[illegible]	[illegible]	[illegible]	[illegible]	[illegible]
D	[illegible]	[illegible]	[illegible]	[illegible]	12.22	12.22	12.22	12.56	[illegible]	[illegible]
E	[illegible]	[illegible]	15.43	[illegible]	[illegible]	[illegible]	17.20	[illegible]	17.69	[illegible]

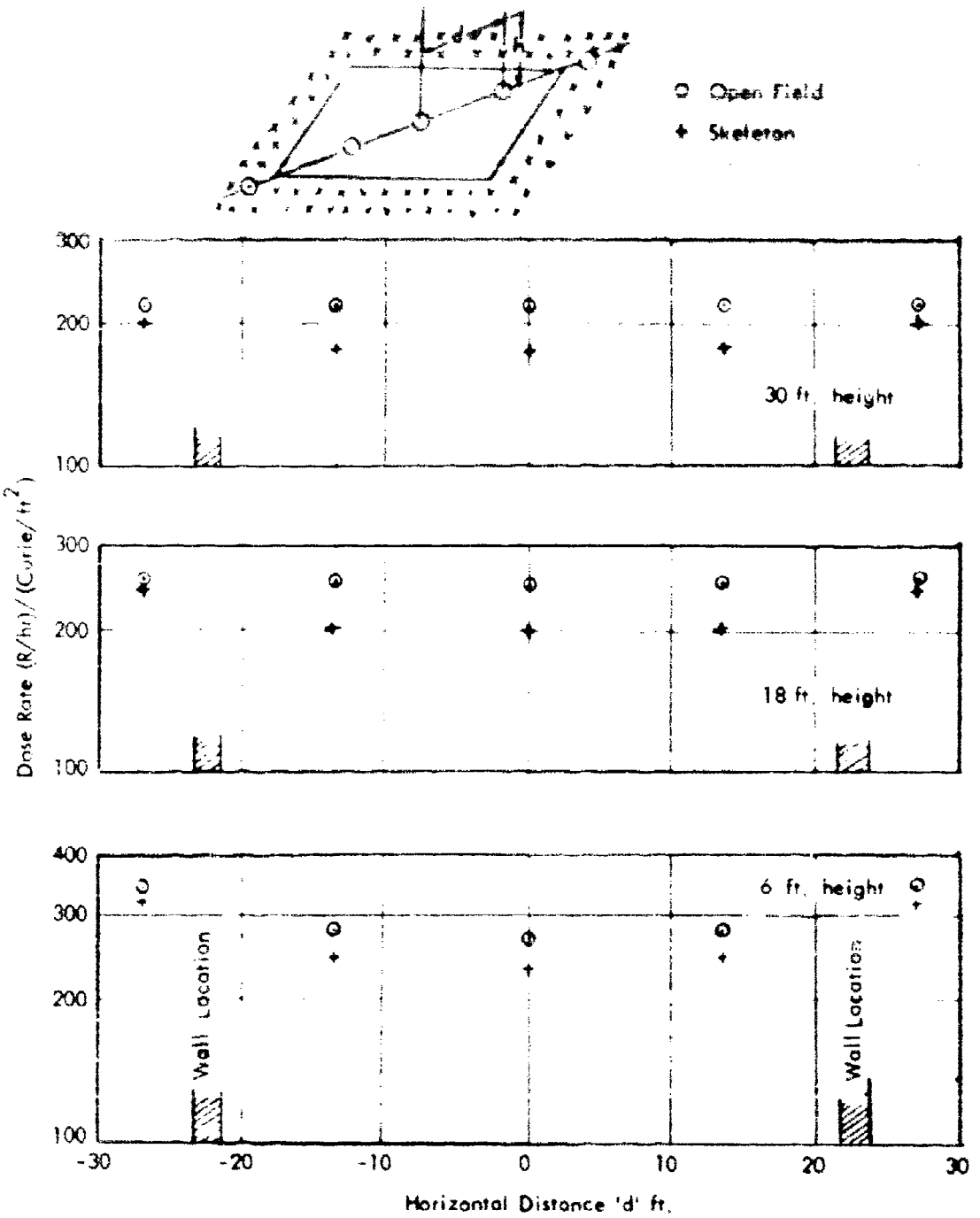

Figure 4.4 - Dose Rate Distribution with Position - Horizontal Diagonal Traverse

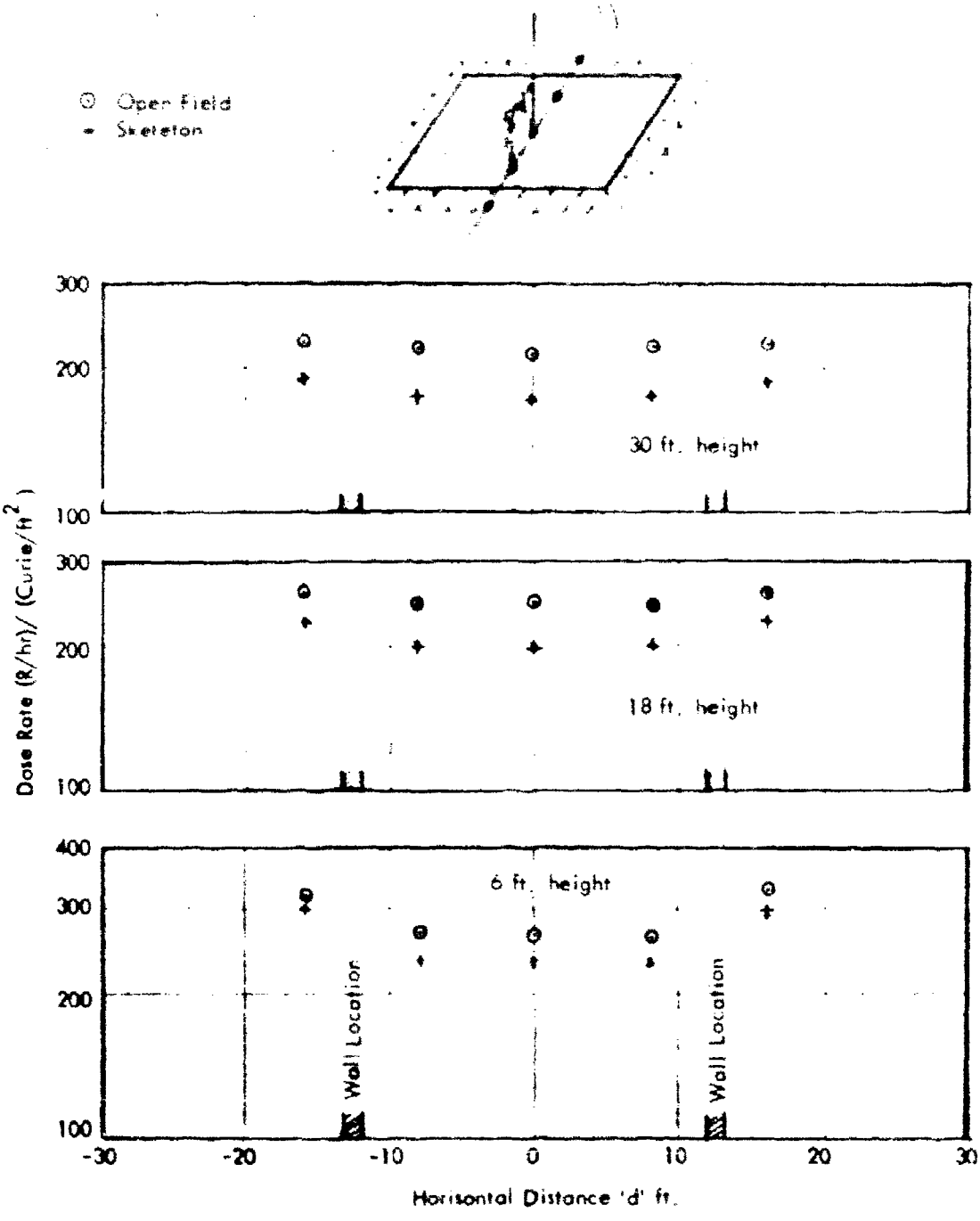

Figure 4.5 - Dose Rate Distribution with Position - Horizontal Fore and Aft Traverse

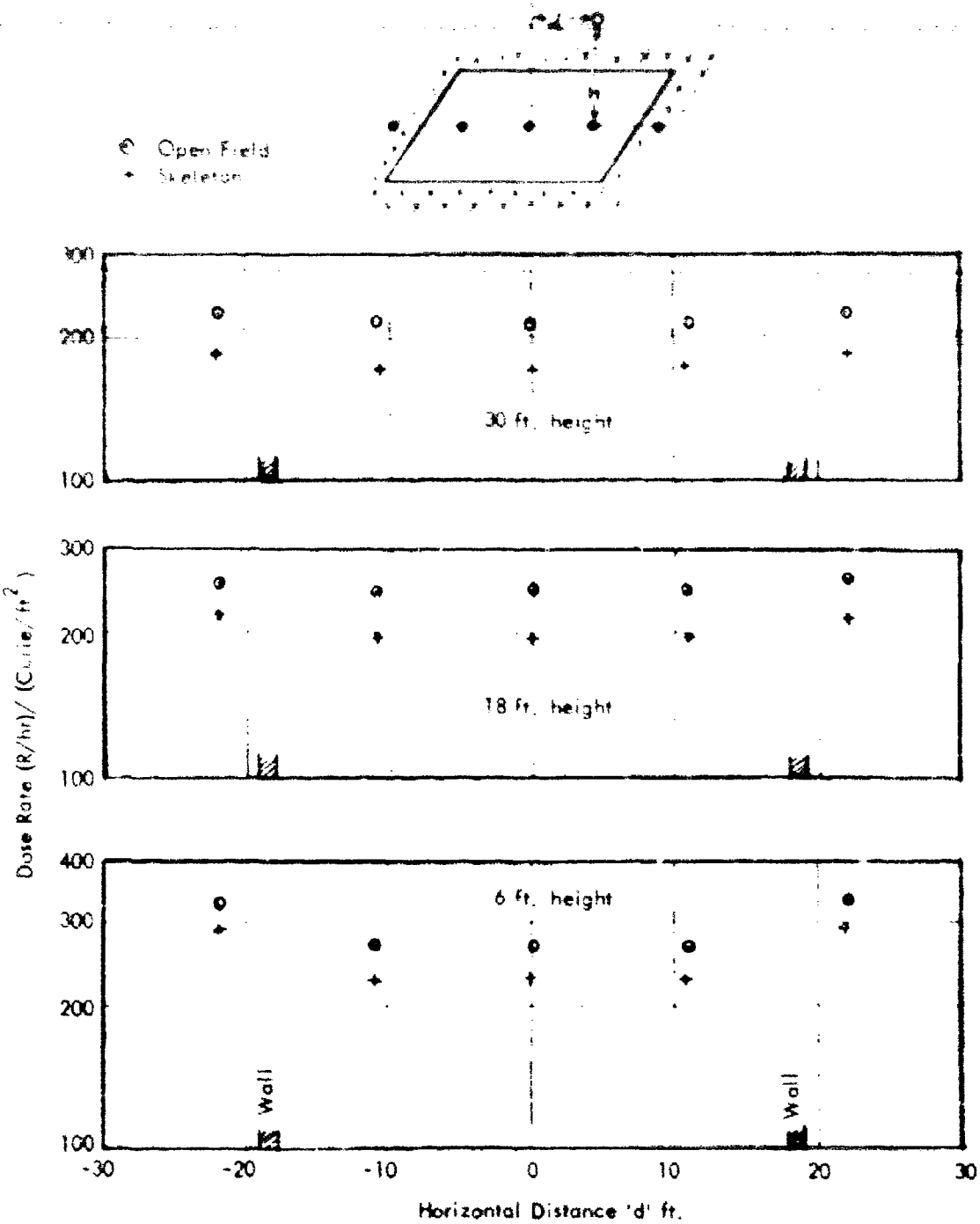

Figure 4.6 - Dose Rate Distribution with Position - Horizontal Side by Side Traverse

Figure 4.7 - Dose Rate Distribution with Position - Vertical Centerline Traverse

CHAPTER 5

ANALYSIS AND INTERPRETATION OF DATA

5.1 INTRODUCTION

In order to gauge the overall effectiveness of a protective structure in a fallout field, a standard "unprotected" position is needed for comparison. The standard unprotected position used for analysis of a structure is a point 3 feet above an infinite, smooth, uniformly contaminated plane. To obtain a quantitative estimate of the protection afforded by a given structure in a real field, the dose rate at any position within the structure is compared to the dose rate that would exist 3 feet above the contaminated plane if the building were absent and the plane were smooth and infinite in extent.

Experimental measurements have been made (1) to determine the open field dose rates from a "real" field, (2) to gather data so that the attenuation introduced by the departure of the field from ideal conditions can be distinguished from the attenuation introduced by a test structure itself, and (3) to evaluate the effects introduced by the steel frame in which test structures will be constructed. Comparisons are made between experimentally determined dose rates and those determined from computational procedures based on idealized conditions.

5.2 DEPARTURE OF THE TEST FIELD FROM IDEAL CONDITIONS

Theoretical calculations[1, 2, 3] of the radiation shielding of a structure are based on the idealized assumption that the structure is surrounded by an infinite, smooth, uniformly contaminated plane. The contaminated area used in the experiments was obviously not a plane in any strict sense. Since the area deviates from the ideal, the path lengths of radiation reaching the detectors from the area are slightly different from the ideal situation. Also because of possible unevenness of the surface, material other than air might be interposed between the source and the detector. It is thus necessary to experimentally determine the effects of ground irregularities for the real

field so that these effects can be taken into account when tests are performed on various structural configurations.

As was stated in Chapter 2 the free field experiment was, of necessity, offset 75 feet from the steel skeleton structure. Upon physical inspection, the two test fields of simulated contamination appeared to be identical. If the two fields are identical, detector readings taken at the center of each field should vary in the same way with the radius of the contaminated area except for the attenuation or back-scattering introduced by the steel skeleton. If the attenuation of the skeleton is approximately constant for all radii of contaminated areas, the curves of dose rate versus radius of contaminated area should be parallel to each other for both skeleton and free field tests. The only locations within the structure where the attenuation is approximately constant are on the first floor. Detector positions on the upper floors are "shadowed" to various degrees by the horizontal floor support structure, and the attenuation to any given source provided by this floor structure is dependent upon the source's location. Figure 5.1 presents both open field and steel skeleton data for center detector locations at heights of 3, 6, and 9 feet. Figure 5.2 presents data taken at identical positions in tests that were not affected by the steel attenuation. (Position 1E Figure 4.2 and 4.3). Inspection of Figure 5.1 and 5.2 indicates that since the curves of cumulative dose rate versus radius of contaminated field are parallel in all cases there exists no significant difference in ground roughness between the "free field" simulated areas of contamination and that surrounding the test structure.

5.3 FAR FIELD CONTAMINATION

It is clearly impossible to extend the simulated areas of contamination to infinite field conditions so that direct comparisons may be made with theoretical results. Previous experiments, however, have indicated that a field extending to about ten times the building height or one mean-free-path radius, whichever is greater, is sufficient to provide most of the dosage that would have been received from a truly infinite field. If estimates of the dose that originates from areas of contamination in the "far field" (beyond the one mean-free-path distance) are added to the experimental

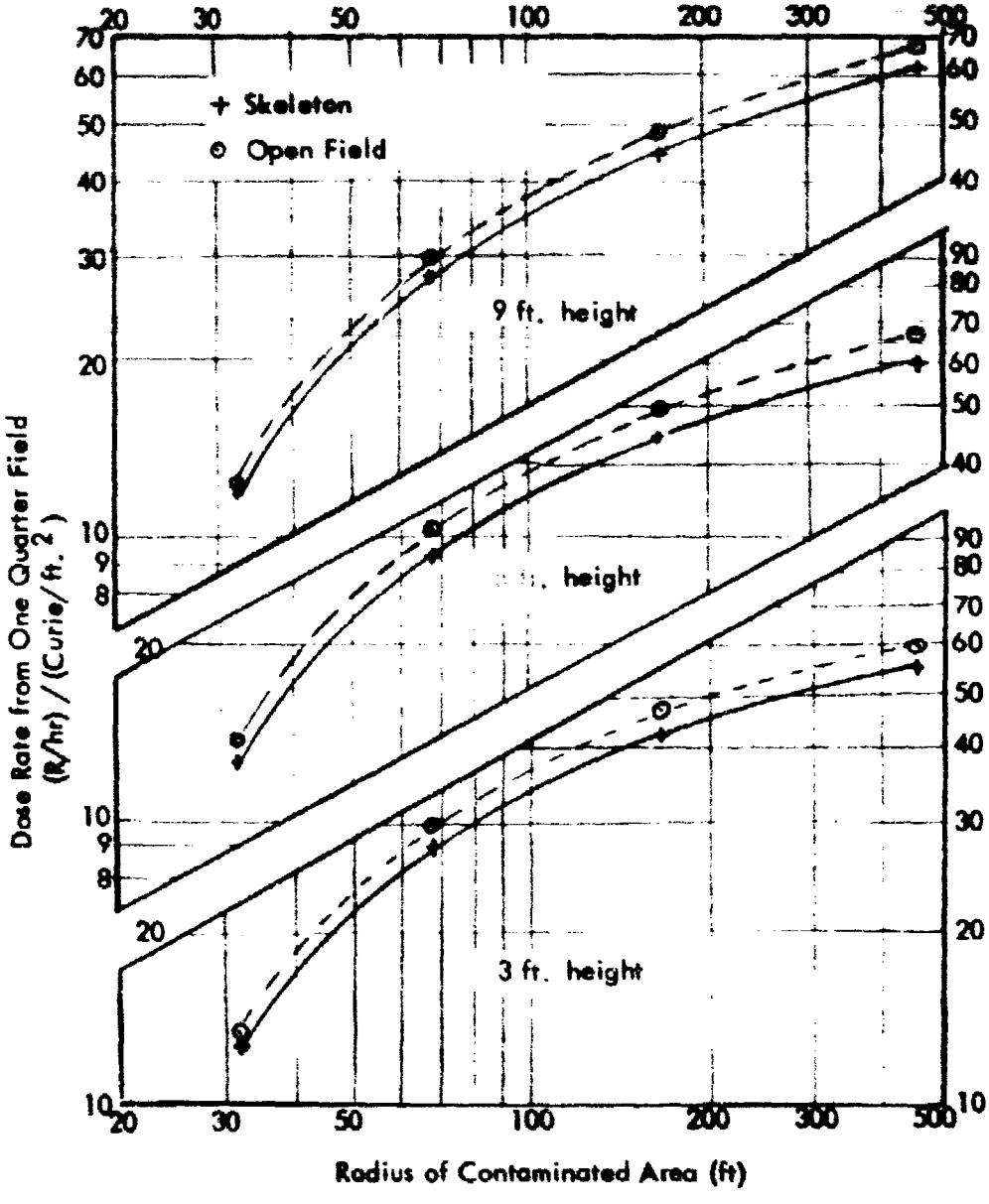

Figure 5.1 - Dose Rate Versus Contaminated Area for Open and Skeleton Fields - Center Position

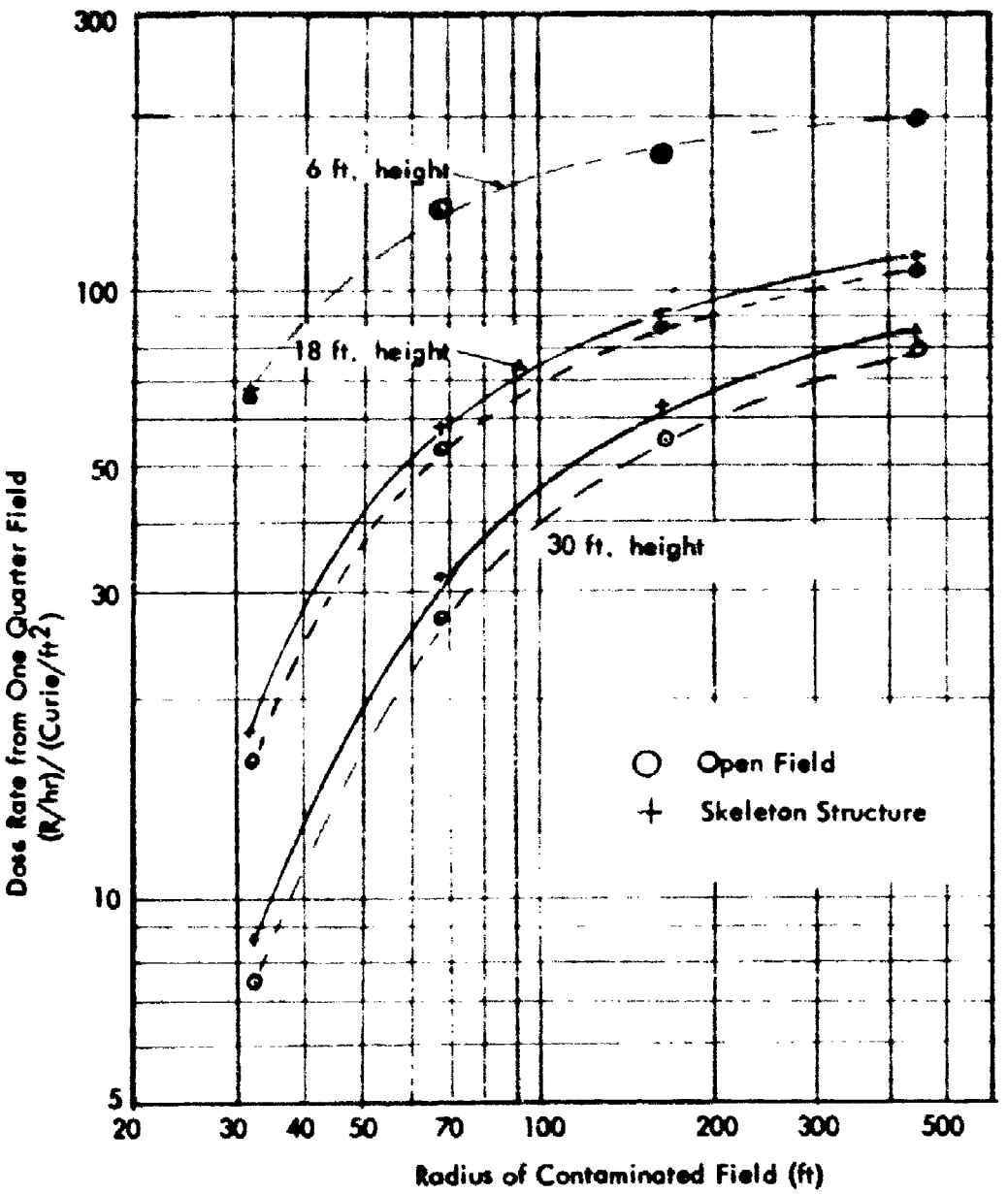

Figure 5.2 - Dose Rate Versus Contaminated Area for Open and Skeleton Fields - Position 1E

data, then results equivalent to infinite field conditions are obtained. An estimate of "far field" dose rate can be made as follows: The total dose arriving at any position at the center of a contaminated annulus of radius r_o, r_i (see Figure 5.3) may be written as:

$$D(h, r_i \rightarrow r_o) = I_o \int_{r=r_i}^{r=r_o} G(x_e, h, a, b \ldots) \frac{2\pi\sigma B(\mu \sqrt{r^2+h^2})\, e^{-\mu \sqrt{r^2+h^2}}}{(r^2+h^2)}\, r\, dr \qquad 5.3.1$$

$D(h, r_i \rightarrow r_o)$ = dose rate at the detector position of interest

h = detector height

r_i = inner radius of the contaminated annulus

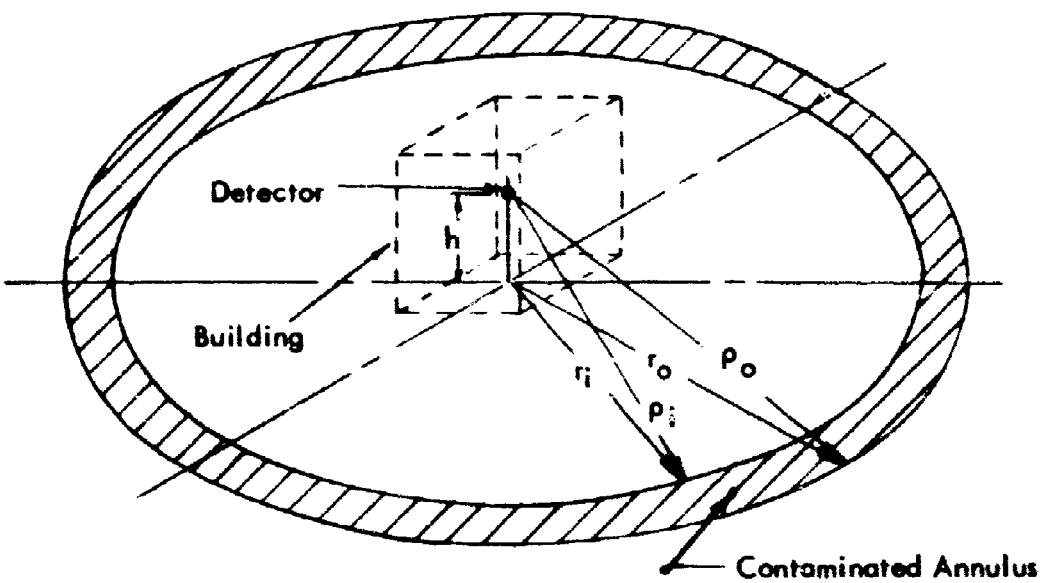

Figure 5.3 – Schematic Diagram of Structure Irradiated by an Annular Contaminated Area

r_o = outer radius of the contaminated annulus

I_o = specific irradiance (R/hr one ft. from one curie source)

$G(x_e, h, a, b...)$ = geometric and barrier shielding introduced by the test structure

x_e, a, b = factors describing the structure

σ = density of contamination curies/ft.^{2}

$B(\mu\sqrt{r^2+h^2})$ = dose buildup factor in air

μ = total linear coefficient for air

If the dose buildup factor is represented as a polynomial and if the geometry and barrier shielding factor $G(x_e, h, a, b,)$ is assumed constant so that it may be removed from under the integral sign, the equation may be integrated. The assumption that the shielding factor is constant for far field radiation is reasonable since the angular and energy distribution (measured at the test structure face) of gamma rays originating from locations at radial distances large with respect to the structure height are nearly independent of radial distance. The attenuation $G(x_e, h, a, b, \ldots)$ afforded by the structure to these gamma rays is thus essentially constant.

The dose buildup factor may be represented by a polynomial expansion such as:

$$B(\mu\rho) = a_o + a_1 \mu\rho + a_2(\mu\rho)^2 + \cdots\cdots$$

where

ρ = actual source to detector distance

μ = total cross section

$a_o, a_1 a_2 \ldots$ = experimentally measured constants

Several investigators[6, 8, 10] have determined these constants, giving values for a, ranging from 0.55 at several feet above the interface to 1.0 at altitudes of fifty feet or more for values of $\mu\rho \geq 0.1$. The simplest expression that adequately fits all

of the existing experimental data at moderate altitudes is that presented in reference (6). This expression is:

$$B(\mu\rho) = 1.0 + 0.55\,\mu\rho \qquad 5.3.2$$

Substituting this expression in equation 5.3.1 and integrating with $G(x_e, h, a, b)$ held constant, the dose rate from an annular contaminated field extending from r_i to r_o becomes

$$D(h, r_i \rightarrow r_o) = 2\pi\sigma I_o G(x_e, h, a, b\ldots)\left[E_1(\mu\rho_i) + 0.55e^{-\mu\rho}i - E_1(\mu\rho_o) - 0.55e^{-\mu\rho}o\right] \qquad 5.3.3$$

where:

ρ_i = slant radius = $\sqrt{r_i^2 + h^2}$

ρ_o = slant radius = $\sqrt{r_o^2 + h^2}$

$E_1(x)$ = exponential integral of the first kind

If the outer slant radius ρ_o is allowed to go to infinity the "far field" dose contamination (that from all sources lying beyond ρ_i) may be calculated in terms of fundamental quantities and the parameter $G(x_e, h, a, b\ldots)$. An estimate of the dose arising from contamination lying beyond the outermost simulated annulus can be obtained by multiplying the dose obtained at each detector position by the ratio of the calculated "far field" dose to that calculated as arising from the last annulus. The ratio of "far field" dose rate to that obtained from the outermost contaminated annulus is thus:

$$R = \frac{D(h, r_o \rightarrow \infty)}{D(h, r_i \rightarrow r_o)} = \frac{E_1(\mu\rho_o) + 0.55\,e^{-\mu\rho_o}}{E_1(\mu\rho_i) - E_1(\mu\rho_o) + 0.55(e^{-\mu\rho_i} - e^{-\mu\rho_o})} \qquad 5.3.4$$

where:

ρ_o = slant distance from the detector to the maximum outer radius of the outermost simulated field

ρ_i = slant distance from the detector to the inner radius of the outer field simulated

h = the detector height

The resultant ratio of "far field" dose (the dose if the field had been contaminated from the outermost radius of the simulated area to infinity) to that obtained from the outermost annulus simulated in the experiment is presented in Table 5.1

TABLE 5.1

RATIO OF "FAR FIELD" DOSE TO THAT OBTAINED FROM AREA 4 or 4A

Dosimeter height (ft.)	Ratio	Dosimeter Height (ft.)	Ratio
1	0.567	21	0.574
3	0.568	24	0.575
6	0.569	27	0.576
9	0.570	30	0.577
12	0.571	33	0.578
15	0.572	36	0.579
18	0.573		

5.4 OPEN FIELD RESULTS

The methods of experimentally simulating an infinite smooth uniformly contaminated plane represent only an approximation of the ideal situation. The experimental field is not infinite in extent, the ground is not a smooth plane in the mathematical sense, and the condition of "uniform contamination" is represented by closely spaced lines of contamination. The major purpose of the open field tests is to evaluate the effect of those approximations on the test results. Spencer[1] has performed an elaborate

series of moments method calculations of the dose rate above such a field contamination with either fallout, Cobalt or Cesium. The results of this calculation, normalized to unity at three foot altitude are presented as a function of height above the plane. Rexroad[8] has performed experiments and French[13] a Monte-Carlo calculation to evaluate the dose-height relationship in terms of the source density actually existing on the ground.

French's results are expressed as the dose buildup factor 3 feet above an infinite plane source of contamination as a function of isotope energy. His value of 1.16 for the mean energy of cobalt radiation (1.25 mev) yields an infinite field dose rate of 453 (R/hr)/(curie/ft^2) three feet above the contaminated plane for standard conditions of pressure and temperature.

Rexroad's evaluation was performed by measuring the dose rate from sources located at different distances from a detector and numerically integrating the results. To eliminate the effects of ground roughness, Rexroad placed his sources slightly above the ground such that no shadowing effects caused by minor variations in terrain height would exist. The results of this experiment are presented in excellent detail in reference (6). Unfortunately there exists some question as to the actual strength of the sources used. Rexroad calibrated his cobalt sources at an 11-foot height with the source and detector approximately six feet apart. Allowance for air and ground scatter was then estimated by placing a small lead shield approximately eight inches thick between the source and detector and reading the scattered dose. The difficulty in such a measurement is that the scatter introduced by the edges of the shield can be greater than the air and ground scatter one is attempting to measure. Thus Rexroad obtains a scatter component of 5.1% of direct beam while Clarke[11] in measurements taken with similar geometry, without the lead shield, reports about 1/2% air and ground scatter. Since the source calibration is dependent on direct beam values alone, Rexroad's source may be as much as 4.6% higher than the quoted value. Also, source strengths are reported using a value of 14.3 Roentgens per hour one foot from a one curie source rather than the currently used value of 14.0. His data must thus be reduced by these two factors, a total of 6.7 percent, if direct comparisons with the data obtained in these present experiments is to be made.

The data obtained from these experiments for center detector locations

is presented in Table 5.2 for each test area. This data, summed to infinity, and that calculated by Spencer, normalized to Rexroad's reduced value of 464 Roentgens per hour 3 feet above an infinite plane field (contaminated to a density of one curie per square foot of cobalt-60) is illustrated in Figure 5.4. Inspection of this figure indicates

TABLE 5.2

DOSE RATE ABOVE AN INFINITE CONTAMINATED FIELD
(R/hr)/(Curie/ft.^{2})

Height (ft.)	Area 0	Area 1A	Area 2A	Area 3A	Area 4A	Far Field (Calculated)	Total
1	225.6	51.0	54.1	52.9	31.7	18.0	433.3
3	159.4	54.0	65.7	65.5	54.0	30.7	429.3
6	105.9	54.2	69.8	74.0	68.6	39.4	411.9
9	73.8	48.4	69.8	74.0	72.1	41.5	379.6
15	40.8	38.0	62.0	74.0	74.4	42.8	332.0
18	31.6	32.6	59.8	75.4	78.5	44.9	322.8
21	25.6	28.3	56.4	75.4	77.3	44.2	307.2
27	15.0	22.0	53.6	72.0	78.5	45.0	286.1
30	12.9	19.2	46.2	70.8	81.4	45.6	276.1
33	10.8	17.6	44.0	70.8	82.6	47.5	273.3
Inner Radius (ft.)	0.0	17.9	32.0	68.0	164.0	452.0	0
Outer Radius (ft.)	17.9	32.0	68.0	164.0	452.0	∞	∞

excellent agreement at all locations except the one and three foot levels. This is to be expected as minor variation in ground terrain (ground rolling effect) would introduce shadowing effects for only the lower detectors. Because of the good agreement between experiment and theory it seems reasonable to use 464 as the standard value of dose rate

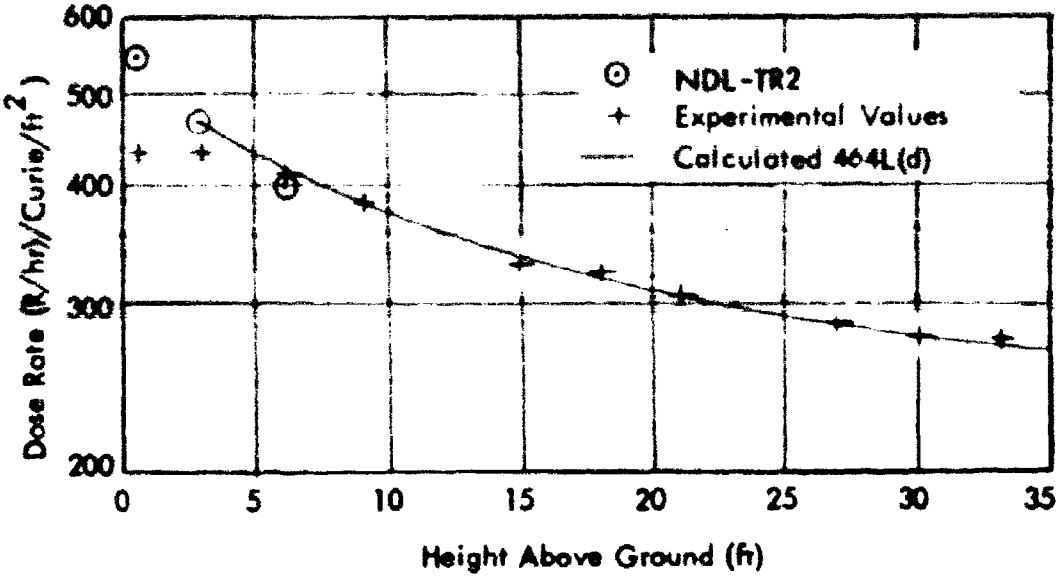

Figure 5.4 - Dose Rate Above an Infinite Contaminated Field

at 3 ft. height in the absence of ground effects for an infinite field contaminated to a density of one curie per square foot of cobalt-60.

Placement of a test structure within a field necessitates the clearance of an area equivalent to the building plan area. The reduction in dose rate at each central location of the open field may be calculated in a straightforward manner by application of the techniques described in the OCD Engineering Manual.[2] In the Engineering Manual the dose rate above a cleared rectangular area is expressed as;

$$\frac{D(h)}{D_o} = L(h) \left[G_d(\omega_1, h) + G_o(h) \right] \qquad 5.4.1$$

where:

D_o = Dose rate 3 ft. above an infinite contaminated field

$L(h)$ = Infinite field dose rate as a function of height h

$G_d(\omega_1, h)$ = Cumulative angular distribution of direct and scattered radiation arising from below the horizon for cobalt radiation.[12]

$G_a(h)$ = Total skyshine radiation contribution for cobalt radiation.[12]

ω_1 = Solid angle fraction of the cleared area as viewed from the detector location

h = Detector height

The function $G_d(\omega_1, h)$ is calculated by summing the direct and scattered radiation entering the detector from all angles extending from $\omega = \omega_1$ to 1, at height 'h'. It thus neglects radiation that might enter a detector by originating outside the area described by ω_1, scattering within the volume defined by ω_1 and the ground and being intercepted by the detector. $G_d(\omega_1, h)$ is thus exact only for the case of ω_1 equal to zero and would be expected to be slightly low elsewhere. It should also be cautioned that the angular distribution of scattered radiation which are summed are calculated from an infinite media – infinite source moments method calculation without a density interface and thus are not exact.

An estimate of the experimentally determined value of $G_d(\omega_1, h)$ may be made from the open field experimental data and equation 5.4.1. This estimate based upon "extrapolated values" of the experimentally determined dose rate above the cleared area (representing the plan area of the test structure) is given in Table 5.3. The

TABLE 5.3

ESTIMATE OF $G_d(\omega, h)$ FROM EXPERIMENTAL DATA

Detector height (ft.)	Solid angle ω_1	Dose rate from a standard field R/hr (1/464 curies/ft^2)	L(h) Ref. 1	$G_d(\omega_1, h)$ calculated from exp. data	$G_d(\omega_1, h)$ calculated from Ref. 12
3	.82	.66	1.0	.57	.55
6	.67	.66	.90	.64	.61
9	.54	.66	.83	.71	.66
15	.34	.63	.74	.74	.71
18	.27	.62	.70	.79	.73
21	.22	.60	.67	.80	.74
27	.16	.59	.62	.86	.75
30	.14	.57	.59	.88	.76
33	.12	.56	.57	.89	.77

experimental data was "extrapolated" back to three foot height to correct for ground roughness using the results of Ref. 1 and 8. It should be noted that the experimentally determined values of $G_d(\omega_1, h)$ are all slightly higher than those calculated from theory as would be expected.

A second method of computation that can be used to calculate the dose rate above a cleared area is stated in reference (1) as;

$$\frac{D(h)}{D_o} = L(\rho) \qquad 5.4.2$$

$$\rho = \text{slant height} = \frac{h}{1-\omega_1}$$

Where the other quantities are defined as before. This expression is developed from the consideration that the equations representing the summed differential angular dose rate from an infinite contaminated field and from an infinite field containing a cleared area are identical except for their limits of integrations when that field is surrounded by an infinite media. The relationship is only approximate when the contaminated plane is also a density interface, since those gamma rays originating at a great distance must travel a long distance to reach the detector over a path which is not far above the interface. These photons thus have a large probability of being deflected into this interface, and when this happens the distance between successive interactions shrink from hundreds of feet to a few inches (if the interface is to be representative of ground), and the probability of absorption at a location far from the detector is increased. The approximate relationship 5.4.2, based upon infinite media conditions with no density interface, would be expected to give a slight overestimate of the dose rate above a cleared area.

The dose rates measured in these experiments above the cleared area in an infinite contaminated field are presented in Figure 5.5 together with those obtained from equations 5.4.1 and 5.4.2. Inspection of this figure indicates that at altitudes above approximately six feet extremely good agreement is achieved. The measured

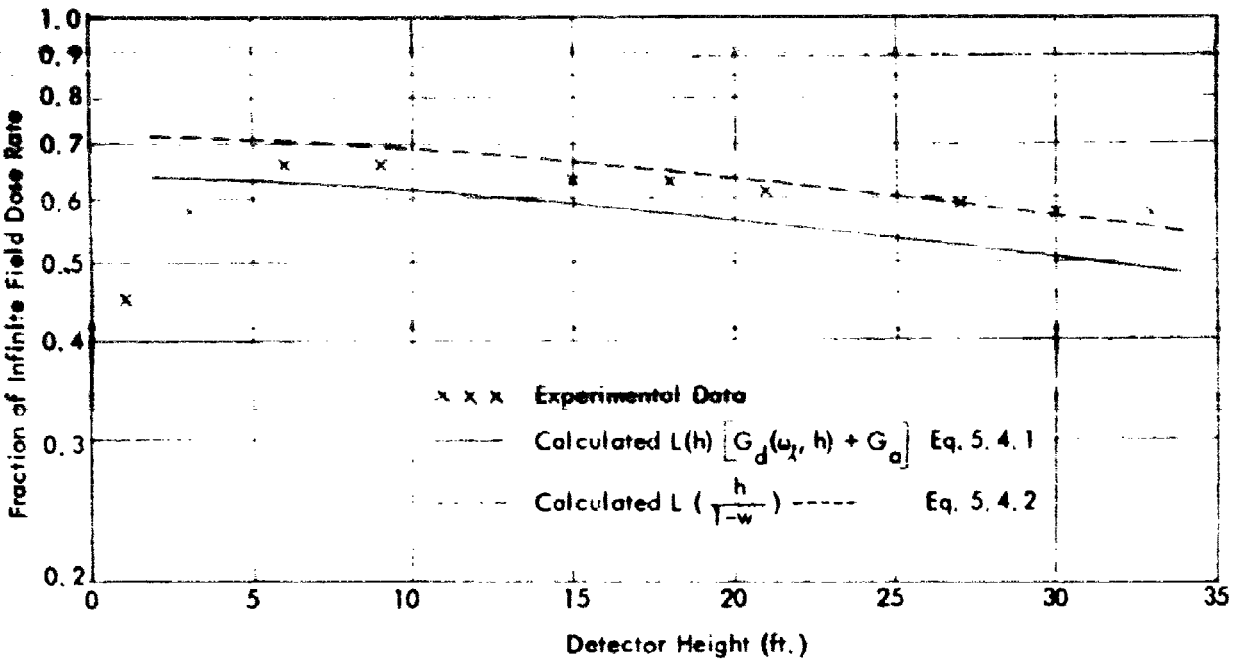

Figure 5.5 - Dose Rate Above a Cleared Rectangle Representing the Building Plan Area

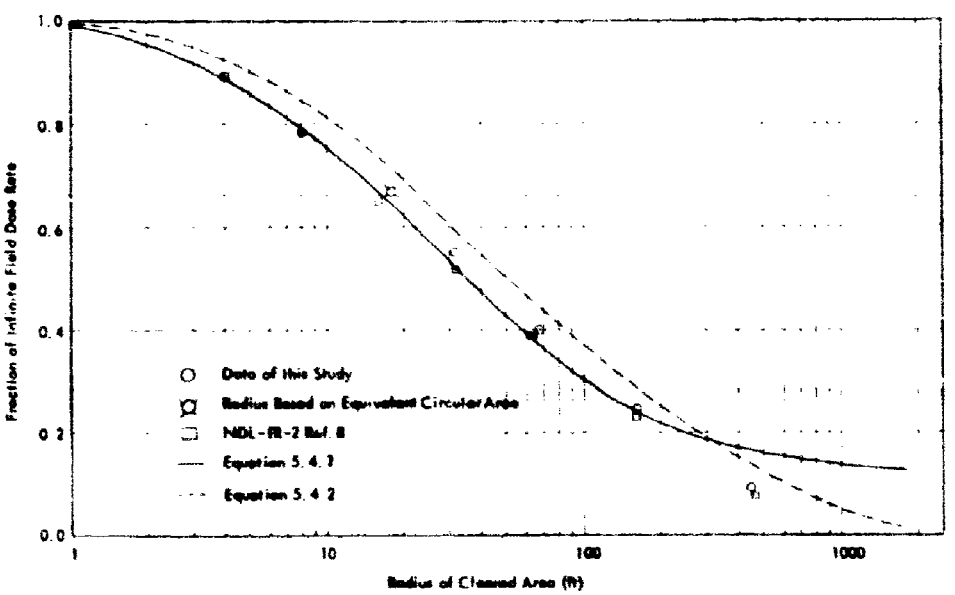

Figure 5.6 - Dose Rate 3 ft. Above a Cleared Circle versus Radius

rates, in general, lie below the results predicted by equation 5.4.2 and above those predicted by 5.4.1 as was expected. Detector readings at low altitudes drop below that predicted by both methods as a portion of the "far field" sources of contamination are hidden by the minor variations in terrain, ("ground roughness").

Equations 5.4.1 and 5.4.2 may be extended to predict the fraction of infinite field dose rate remaining after any given area has been cleared. It should be noted that in equation 5.4.1 the skyshine term is assumed unaffected by the area cleared, and since this assumption is true only for small areas, this relationship is not a good representation of the case for detectors located above large cleared areas. Plots of equations 5.4.1 and 5.4.2 are presented for 3 ft. altitude in figure 5.6 together with the data of Rexroad and data from these experiments. The values presented for these experiments were obtained by plotting the dose rate versus altitude from each experimental area and extrapolating to the altitude of three feet. The effect of ground roughness at the lower altitudes (below about six feet) is thus removed so that direct comparisons may be made between theory, these experiments, and previous experiments.

As can be seen from the figure excellent agreement between the theoretical and experimental data exists. Equation 5.4.1 provides an underestimate of the dose for small radii clearings and an overestimate for large radii as was expected. Similarly, equation 5.4.2, as expected, provides an overestimate of the dose rate for any clearing size.

5.5 COMPUTATION OF SKELETON STRUCTURE

The Engineering Manual[2,3] type calculations give the reduction factor at a detector inside a structure surrounded by an infinite plane field of contamination. They apply to cases where the walls and floors have uniform thicknesses. The reduction factor for the case of a typical structure is the product of a barrier factor which depends on the thickness of the walls and a geometry factor which depends on the distance of the detector from the various walls.

The usual approach to the problem of shielding analysis is to consider a simple structure with only one type of wall construction. The steel structure investigated in this report, on the other hand, consisted of a framework of 8 inch floor beams and

8 and 14 inch vertical columns. The spacing between beams was 4 feet. The Engineering Manual method is not therefore directly applicable to this experiment. However, in an attempt to account for the dose rate distribution in the skeleton structure, a modification of the Engineering Manual analysis has been made and is presented in this report.

The method given in the manual to analyze a structure composed of different types of wall construction is the azimuthal sector approach. The azimuthal sector approach is described in detail in Reference 2. It consists of calculating the azimuthal sectors subtended by the detector for each different wall type, the calculation of a fictitious building in which all walls are of this type, and then a summation of these results weighted by their azimuthal fraction. The calculations for ground contribution for each fictitious building are completed in the usual manner and then adjusted by the azimuthal fraction which a wall occupies in the actual structure.

While a method of analyzing a structure with different wall construction is proposed in the manual no mention is made of a structure with different floor construction.* Our first attempt to calculate the dose rate in the steel structure consisted of smearing the horizontal floor beams. The azimuthal sector approach was used on the vertical columns forming the walls.

In this calculation, only detectors at the center of the steel structure were considered. The first step is to calculate the angle subtended by the detector for each individual vertical wall beam as illustrated in Figure 5.7. Next, angles from each azimuthal sector are summed and divided by the total azimuthal angle to obtain azimuthal fractions. The building being symmetrical, the calculations are made for only one quadrant. Defining A_z as the decimal fraction of blocked area, and $1-A_z$ as the fraction of open area in the wall, the resultant calculations showed $A_z = 0.3$ and $1-A_z = 0.7$. The effective mass thickness of the vertical beams was calculated as follows:

$$x_e = \frac{W\left(2\,\frac{Z}{A}\right)}{L\,A_z} \qquad 5.5.1$$

where:

x_e = effective mass thickness for vertical columns in the quadrant

*The reason for this is that floor systems are usually uniform and in most common shielding situations the relative dose contribution through the floor is quite small.

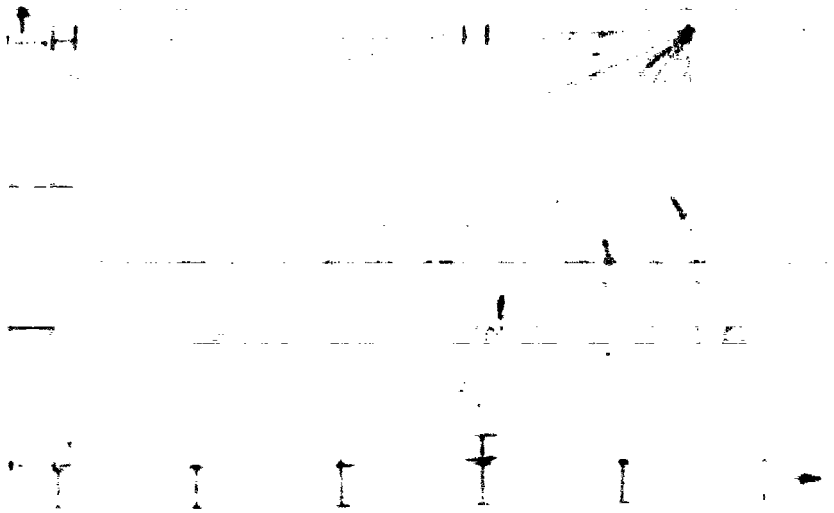

Figure 5.7 - Computation of Azimuthal Sectors

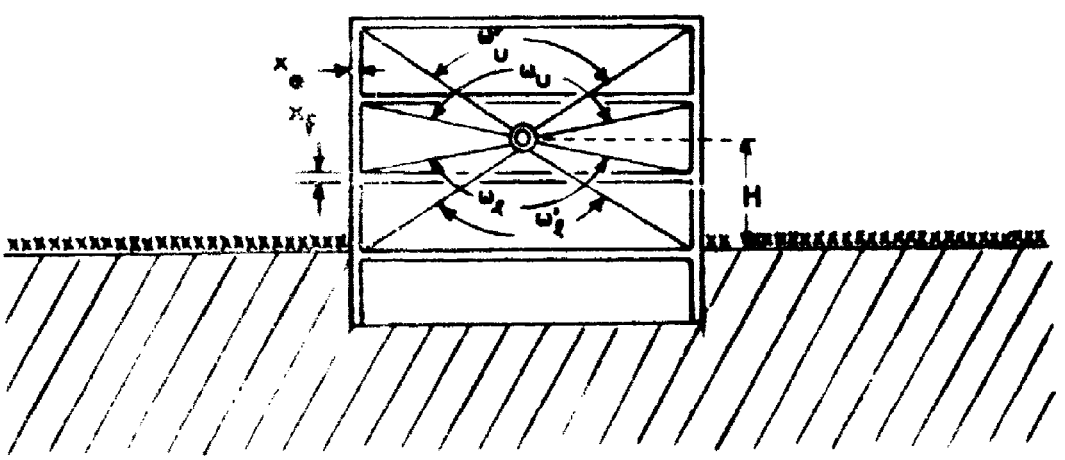

Figure 5.8 - Structure Elevation Illustrating its Geometry

W = pounds per foot of height of all vertical steel columns

$(2\frac{Z}{A})$ = ratio of atomic charge to atomic number for steel

L = total perimeter of building plan

A_z = fraction of structure occupied by vertical steel columns as viewed by the detector

With the above information we can proceed with the functional equations that describe the calculation of dose rate within the steel structure. The functional equations using the notation of Ref. 2, 3 are given below (see Figure 5.8).

Ground contribution to the detector through the walls of the same story as the detector:

$$C_{g_D} = A_z \left\{ \left[G_d(\omega_1, h) + G_a(\omega\mu) \right] (1 - S_\omega) + \left[G_s(\omega\mu) + G_s(\omega_1) \right] S_\omega E \right\} B_e(x_e, h)$$

$$+ (1 - A_z) \left[G_d(\omega_1, h) + G_a(\omega\mu) \right] B_e(x_e = 0, h) \qquad 5.5.2$$

Ground contribution to the detector through the walls of the story below the detector:

$$C_{g_B} = A_z \left\{ \left[G_d(\omega_1', h) - G_d(\omega_1, h) \right] (1 - S_\omega) + \left[G_s(\omega_1') - G_s(\omega_1) \right] S_\omega E \right\} B_e(x_e, h)\, B_o(x_f)$$

$$+ (1 - A_z) \left[G_d(\omega_1', h) - G_d(\omega_1, h) \right] B_o(x_f)\, B_e(x_e = 0, h) \qquad 5.5.3$$

Ground contribution to the detector through the walls of the story above the detector:

$$C_{g_A} = A_z \left\{ \left[G_s(\omega_U') - G_s(\omega_U) \right] S_\omega E + \left[G_a(\omega_U') - G_a(\omega_U) \right] (1 - S_\omega) \right\} B_o'(x_o) B_e(x_e, h)$$

$$+ (1 - A_z) \left[G_a(\omega_U') - G_a(\omega_U) \right] B_o'(x_o) B_e(x_e, = 0, h) \qquad 5.5.4$$

Total ground contribution to the detector:

$$C_g = C_{g_D} + C_{g_B} + C_{g_A} \qquad 5.5.5$$

where

$G_a(\omega)$	=	the directional response of atmospheric-scattered radiation
$G_s(\omega)$	=	the directional response of wall-scattered radiation
$G_d(\omega, h)$	=	the directional response of direct radiation
ω	=	a solid angle fraction (solid angle/2π) (see Figure 5.8)
h	=	detector height above ground
S_ω	=	the fraction of radiation scattered by the wall
E	=	an eccentricity factor depending upon length-to-width ratio
$B_e(x_e, h)$	=	the barrier shielding introduced by a vertical wall of thickness x_e at height h above the ground
$B_o'(x_f)$	=	the barrier shielding introduced by an overhead mass thickness x_f to atmospheric or wall-scattered radiation
$B_o(x_f)$	=	the barrier shielding introduced by the floor below the detector
A_z	=	percentage of open area occupied by the vertical columns as viewed by the detector

It should be noted that these equations are applicable only to a structure of an infinite number of stories where radiation from floors more distance than those

immediately above and below the detector have no significant effect on the reading. In the real situation this is in general true except for detector locations on floor near the top of the structure. In this instance an additional term must be added to the equations to account for the skyshine entering through the building roof.

Although shielding calculations in the Engineering Manual[2,3] are based upon 1.12 -hour fallout spectra, while the skeleton results were obtained using cobalt-60 as a fallout simulant, Spencer[1] presents similar curves for both cobalt-60 and fallout spectra so that direct computations can be made of the test conditions where cobalt is used. For the computations the methods and nomenclature of the Engineering Manual together with functions evaluated for cobalt-60 in Reference 1 were used.

The results of a series of computations using equations 5.5.1 through 5.5.5 together with the assumption that the floor mass may be smeared is presented in Table 5.4 together with that obtained directly from this experiment. Note that equation 5.5.2 reduces to that of 5.4.1 for the case of no building (here $B_e(x_e = 0, h) \equiv L(h)$).

TABLE 5.4

THE DOSE RATE FROM GROUND BASED SOURCES OF RADIATION
(R/hr from a Standard Field)*

	Open Field			Skeleton		
Detector height (ft.)	Experimental (R/hr)	Calculated (R/hr)	Ratio Cal/exp.	Experimental (R/hr)	Calculated (R/hr)	Ratio Cal/exp.
1	.45	--	--	.46	--	--
3	.59	.64	1.09	.54	.55	1.02
6	.66	.63	.96	.57	.54	.95
9	.66	.62	.94	.53	.53	1.00
15	.63	.59	.94	.47	.34	.72
18	.62	.57	.92	.50	.35	.70
21	.60	.56	.93	.50	.38	.76
27	.59	.53	.90	.42	.26	.62
30	.57	.50	.88	.45	.30	.67
33	.56	.49	.88	.46	.31	.67

* A standard field is defined as that field which if smooth and infinite in extent would produce 1 R/hr at an altitude of 3 feet above it. ($\frac{1}{464}$ curies/ft^2 Co-60).

Agreement between calculation and experiment is excellent for the open field and on the first floor of the skeleton structure (with the calculated data generally falling slightly lower than that measured) but not very good for the upper floors. From the discussion of Section 5.4 the predicted dose rates are expected to fall slightly below those measured for above ground positions. This effect can be attributed to the fact that the quantity $G_d(\omega)$ is computed neglecting the radiation that scatters to the detector from the air volume defined by the detector and the floor plan area. The effect of neglecting this component should grow larger with increasing dosimeter height as this volume contains more and more air. Thus, with the exception of the detector values in the lowermost locations which are affected by ground roughness, the difference between experimental and calculated values is as expected from theory.

Since good agreement is shown on the first floor of the steel structure but not on the upper floor locations it is evident that the proposed method of handling floor inhomogeneity by smearing the mass of the floor and computing a barrier factor based on this smeared mass is not adequate. A second approximate formulation for the barrier factor, similar in some respects to the azimuthal sector method used for vertical barriers, may be made as follows. The equivalent barrier factor for an inhomogenous floor is set equal to the sum of the barrier factors for each homogenous portion of the floor, weighted by the fractional area of that section of the floor. Thus;

$$B_o(x_f) = B_o(x_{f1})\,A_1 + B_o(x_{f2})\,A_2 + \cdots \qquad 5.5.6$$

where

$B_o(x_f)$ = weighted barrier factor for inhomogenous floors

$B_o(x_{fn})$ = barrier factor of the n^{th} area of the floor

A_n = fraction of total floor area of the n^{th} area of the floor

Similarly, $B'_o(x_f)$, the barrier factor for an overhead mass can be computed. When these new calculations are performed, the barrier factors are changed from 0.29 to 0.768 for B'_o and from 0.27 to 0.760 for B_o. These values are quite near what is actually experienced in the structures. The dose rate as illustrated in Figure 5.9 just above and below

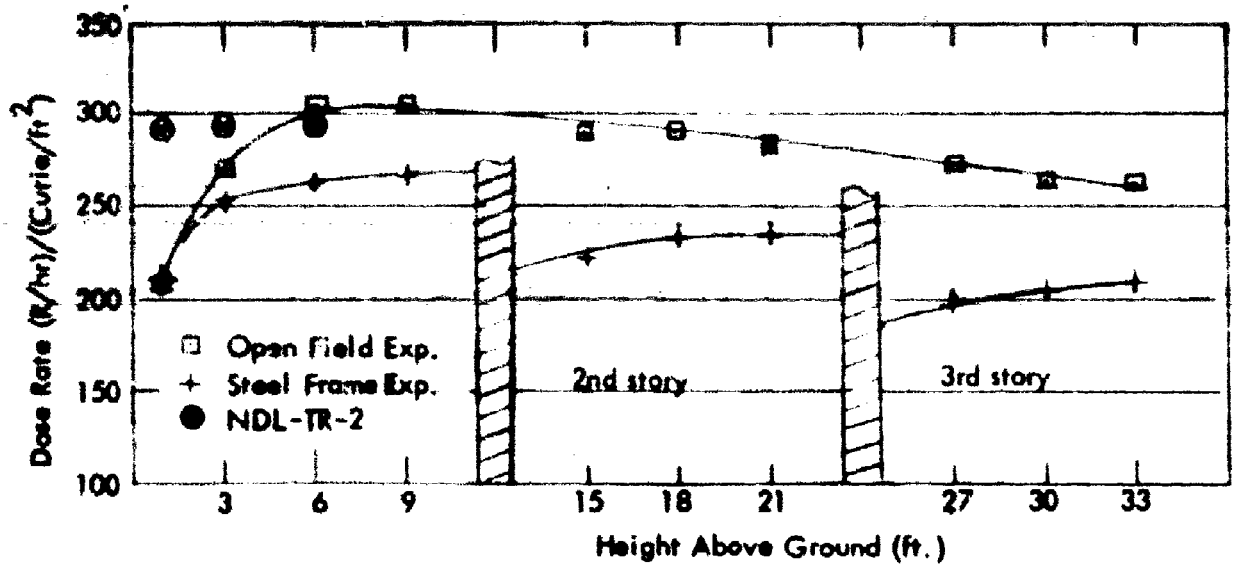

Figure 5.9 - Dose Rate Above the Cleared Rectangular Area Representing the Building Plan Area - Open Field and Steel Skeleton

the structure floors varied by about 0.75 to 0.85. If the new calculated values are now substituted in equations 5.5.3 and 5.5.4 in place of the smeared barrier factors for floor and ceiling, the computed dose is found to agree quite well with that experimentally measured. This is illustrated in Table 5.5.

Note that the calculated dose now shows fairly good agreement with that measured - the dose being in general slightly lower as expected. Table 5.3, 5.4 and 5.5 does, however, mask the effect of ground roughness on the lower experimental values. A more valid comparison may be made by comparing the ratio of calculated values of the steel skeleton divided by the calculated values of the open field with a similar ratio computed from the experimental data. This is presented in Table 5.6. This ratio "removes" not only the effect of ground roughness but also the fact that G_d underestimates the direct radiation component in the calculation (see Section 5.4).

The extremely good agreement shown (both in magnitude and variation with detector height) in Table 5.6 between experimental and computed ratios indicates that the computational method represented by equations 5.5.1 through 5.5.6 is valid and quite accurate. The major inaccuracy of this method for "thin" structures is caused

TABLE 5.5

THE DOSE RATE FROM GROUND BASED SOURCES OF RADIATION BY MODE OF TRANSMISSION
(R/hr From a Standard Field)

Detector height (ft.)	Dose through the same story Eq. (5.5.2)	Dose through ceiling using $B_o'(x_f)$ (Eq. 5.5.4)	Dose through floor using $B_o(x_f)$ (Eq. 5.5.3)	Total Dose	Dose through ceiling using $\underline{B_o'(x_f)}$ (Eq. 5.5.4)	Dose through floor using $\underline{B_o(x_f)}$ (Eq. 5.5.3)	Total Dose using (Eq. 5.5.6)	Total Dose Exp.
3	.532	.005	--	.54	.014	--	.55	.54
6	.516	.007	--	.52	.019	--	.54	.57
9	.490	.013	--	.50	.034	--	.53	.53
15	.275	.004	.056	.34	.011	.165	.45	.47
18	.318	.006	.031	.35	.016	.092	.43	.50
21	.353	.010	.022	.38	.027	.068	.45	.50
27	.201	.003	.052	.26	.008	.151	.36	.42
30	.267	.004	.032	.30	.011	.094	.37	.45
33	.285	.007	.022	.31	.019	.065	.37	.46

TABLE 5.6

RATIO OF SKELETON DOSE RATE TO THAT OBTAINED IN THE OPEN FIELD

Detector height (ft.)	Floor	Experimental	Shielding* Element	Calculated (using 5.5.6)
3	1	.93	C	.86
6	1	.84	C	.85
9	1	.88	C	.85
15	2	.76	C, H	.76
18	2	.80	C, H	.75
21	2	.83	C, H	.90
27	3	.72	C, H	.69
30	3	.79	C, H	.74
33	3	.80	C, H	.76

* C refers to vertical columns, H refers to horizontal beams. Item of probable dominance is underlined.

by the fact that $G_d(\omega_1, h)$ underestimates the "direct" radiation for values of ω_1 (the solid angle fraction of the cleared area) greater than 0.

As a further test of the use of the area weighted barrier factor for the floor and ceiling attenuation, a calculation was performed to determine the dose rate at an off center position at 15, 18, and 21 foot heights. Because of the complexity of the calculation only one position at three detector heights were computed. This position 3B or 3D (see Figure 4.3) was on the longitudinal centerline of the building and offset eight feet from the center. The off center computation was performed using the "position variation" method described in Reference 2. This procedure involves dividing the building into quadrants surrounding the detector location and calculating the ground contribution for each quadrant by assuming that the detector is at the center of a fictitious structure four times the size of each quadrant. The total contribution for all four fictitious structures are then added and the sum divided by four. The functional equation describing each radiation component has been previously presented as equations 5.5.1 through 5.5.6.

The results of this computation are presented in Table 5.7 together

TABLE 5.7

DOSE RATE AT POSITION 3B or 3D FROM A FULL STANDARD FIELD

Detector height (ft.)	Experimentally determined dose rate R/hr	Calculated dose rate R/hr using Eq. 5.5.6	Calculated dose rate using smeared floors and ceiling
15	0.48	0.46	0.40
18	0.50	0.45	0.40
21	0.49	0.44	0.39

with the experimental data obtained from this present program.

Inspection of this table shows that the floor attenuation as determined by equation 5.5.6 is much more accurate than that obtained by using a "smearing" technique for off center as well as center locations. The slight variation between calculated and experimentally measured values of dose rate can probably be attributed to the fact that the theoretical value of the "direct" radiation $G_d(\omega_1, h)$ is lower than that actually experienced (see Section 5.4).

CHAPTER 6

CONCLUSIONS AND RECOMMENDATIONS

6.1 GENERAL

The purpose of this study has been three fold; first to perform a series of standard experiments designed to "calibrate" the radiation test field of the Protective Structures Development Center; secondly to obtain data upon the variation of dose rate with height to greater heights than previously measured; and thirdly to determine the best computational procedures for handling the inhomogeneity introduced into a test structure by its supporting skeleton. Two major test series were undertaken to achieve these goals. The first series of tests consisted of measuring the dose rate near the center of a contaminated field of 452 foot radius both with and without a cleared area representing the test structure plan area. The second series of tests consisted of measuring the dose rate at identical positions from a duplicate contaminated field surrounding the steel skeleton of the test structure.

6.2 CONCLUSIONS

The major conclusions that can be drawn from this work may be summarized as follows:

1. The dose rate at standard conditions of pressure and temperature ($P = 760_{mm}$, $T = 32^{\circ}F$), three feet above an infinite field contaminated to a density of one curie of Cobalt-60 per square foot, and in the absence of ground roughness is 464 Roentgens per hour. This value agrees well with that previously measured.

2. The decrease in dose with height, neglecting ground roughness effects, agreed well with that predicted by the moments type calculations of Spencer (Ref. 1).

3. The minor variation from flatness of the experimental field at the Protective Structures Development Center causes the dose rate to be reduced by approximately 0.68, 0.88 and 0.97 at one, three and six foot heights respectively.

4. The agreement between theoretical and experimental values of the

dose rate above a cleared area representing the test building plan area is within 12 percent.

5. The experimentally determined values of the cumulative angular distribution function $G_d(\omega, h)$ are as much as 14 percent higher than calculated values. This is to be expected since the theoretical calculations neglect radiation scattering to the detector from the air volume bounded by the detector and the cleared area.

6. The predicted dose rate reduction obtained 3 feet above a uniform contaminated field by clearing a circle of radius r (solid angle fraction ω) as predicted by the theoretical relationship $L\left(\frac{d}{1-\omega}\right)$ is conservative; and as predicted by the relationship $L(h)\left[G_d(\omega) + G_a\right]$ is not conservative for radii less than about one mean free path.

7. The attenuation effects introduced by the steel skeleton of the test structure may be predicted to good accuracy using a modified form of the "Engineering Manual"[2, 3] style calculations.

8. The azimuthal sector method of computing the effect of variations in wall thickness is accurate to within approximately ten percent.

9. The method found best to represent the effects of inhomogeneities in floor and ceiling slabs (for the case of very thin floors) is that of computing an overall barrier factor by summing the area weighted barrier factors for each section of uniform mass density. Thus;

$$\overline{B_o(x)} = \sum_{n=1}^{i} \frac{A_n B_o(x_n)}{A}$$

where

$\overline{B_o(x)}$ = effective floor or ceiling barrier factor

A = total floor area $(ft.)^2$

A_n = the area of the floor having a mass density x_n $(ft)^2$

x_n = the mass density of the n^{th} area lbs/ft^2

$B_o(x_n)$ = the attenuation introduced by a floor or ceiling of mass density x_n

i = the total number of floor or ceiling areas of different thickness

6.3 RECOMMENDATIONS

The major recommendations resulting from this study are that;

1. The function $L\left(\frac{d}{1-\omega}\right)$ be used as a conservative estimate of the dose rate above a cleared area.

2. A further study should be made to accurately determine the values of the cumulative angular distribution parameter for direct radiation, $G_d(\omega, h)$.

3. The "area weighting" technique of computing barrier factors for inhomogenous roof and floor slabs should be investigated further to determine its applicability over a wide range of floor thickness variations.

4. The value of 464 R/hr be used as the standard value for the dose rate above an infinite smooth plane contaminated to a density of one curie per foot squared of cobalt-60 radiation.

REFERENCES

1. Spencer, L. V., "Structure Shielding Against Fallout Radiation from Nuclear Weapons", NBS Monograph 42 (1 June 1962)

2. OCD PM 100-1, "The Design and Review of Structures for Protection from Gamma Radiation", (Dec. 1963)

3. Eisenhauer, Charles, "An Engineering Method for Calculating Protection Afforded by Structures Against Fallout Radiation", NBS-76 (July 1964)

4. "Calculation of Protection Factors for the National Fallout Shelter Survey", NBS 7539 (July 1962)

5. Auxier, J. A., V. O. Buchanan, C. Eisenhauer, and H. Menker, "Experimental Evaluation of the Radiation Protection Afforded by Residential Structures Against Distributed Sources", AEC-CEX 58. 1 (Jan. 1959)

6. Clarke, E. T., J. F. Batter, A. L. Kaplan, "Measurement of Attenuation in Existing Structures of Radiation from Simulated Fallout", TOB, 59-4 (April 1, 1959)

7. Batter, John F., A. W. Starbird, "Planning Document for the Radiation Test Facility of the Protective Structures Development Center", TOB 63-4 Revised April 1963

8. Rexroad, R. E. and M. A. Schmoke, "Scattered Radiation and Free Field Dose Rates from Distributed Cobalt-60 and Cesium 137 Sources", NDL-TR-2 (Sept. 1960)

9. Batter, J. F., "Cobalt and Iridium Buildup Factors Near the Ground/Air Interface", Trans. Amer. Nuclear Soc., Vol. 6, No. 1, Pg. 198, (June 1963)

10. Berger, M. J., "Calculation of Energy Dissipation by Gamma Radiation Near the Interface Between Two Media", J. Appl. Phys. 78, 1502 (1957)

11. Clarke, E. T., and J. F. Batter, "Gamma-Ray Scattering by Nearby Surfaces", Trans. Amer. Nuclear Soc., Vol. 5, No. 1, 223 (June 1962)

12. Ledoux, J., Private Communication (May 1964)

13. French, R. L., "Gamma-Ray Energy and Angular Distributions Above an Infinite Fallout Field", Radiation ResearchAssociates, Inc., RRA-T43 (May 1964)

APPENDIX A

PUMP CALIBRATION

Rate of fluid output from the Hills-McCanna metering type pump can be varied by changing the speed control setting on the Vickers variable-speed drive and/or changing the piston stroke length. For most operations the required pump output can be obtained with full piston stroke (1-1/4 inches) for each of the four pump feeds and varying output with the variable speed drive only. However, for flow rates less than 0.02 lb/sec the pump stroke must be shortened in addition to reducing output RPM of the variable speed drive.

Output of the pump for different variable speed drive positions and pump strokes were measured by weighting the amount of fluid discharged over known time intervals. This measured output converted to a pound per second basis as well as to equivalent fluid velocity within a 3/8 inch I.D. tube is shown in Figure A-1.

During a series of "dummy source" check runs on the "open field" and the "structure" tubing areas, data was taken of the measured dummy source velocity through the tubing versus variable speed drive setting as well as on actual times (Figure A-2) required to push the dummy source through each of the areas for several variable-speed drive settings. Additional points were added to these curves as exposure runs were made with the Co-60 sources. Velocity of the dummy source in the tubing was measured by placing a 100 foot tape beside the tubing and timing the passage of the "dummy" over a known distance.

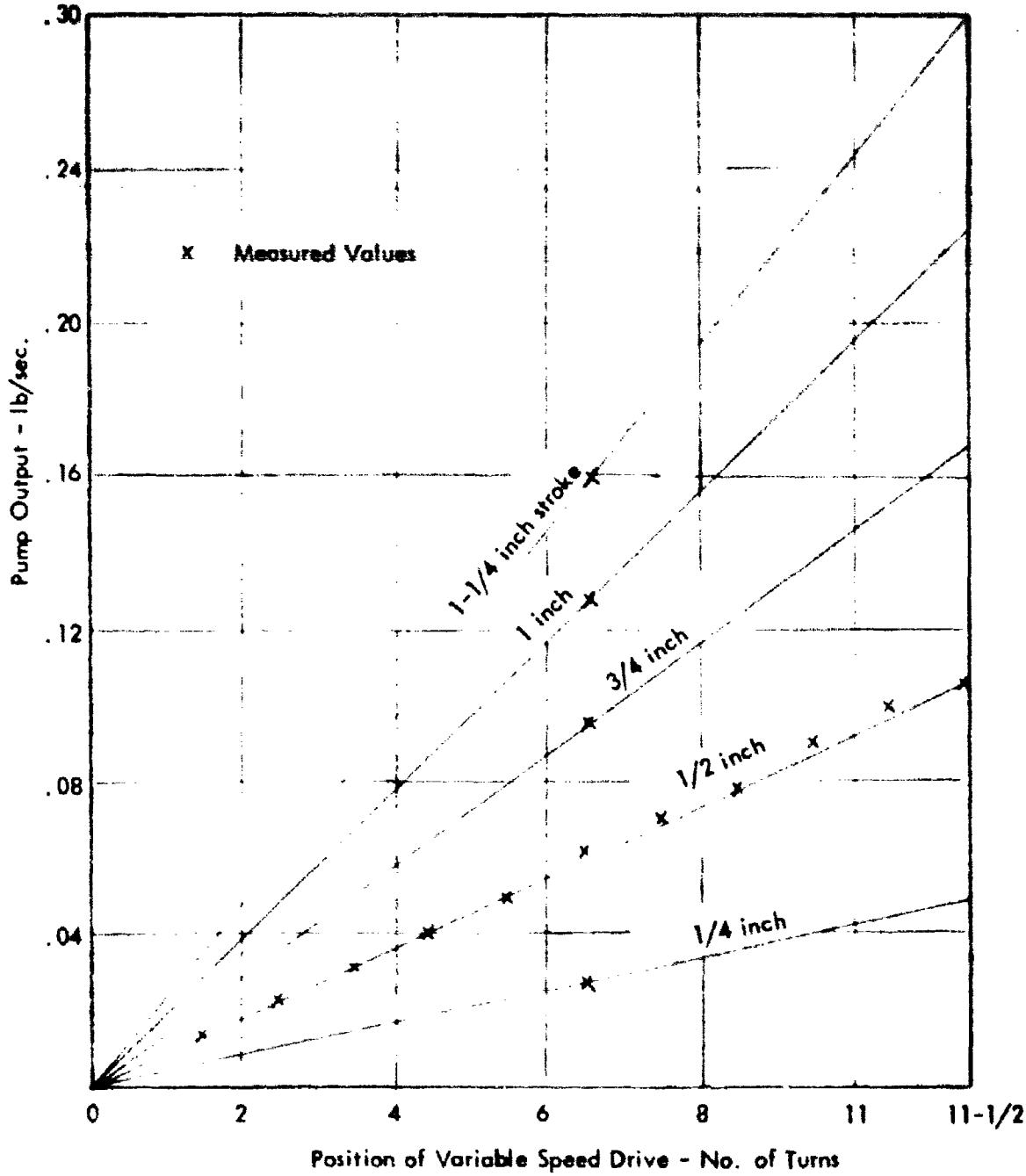

Figure A-1 - Pump Characteristics

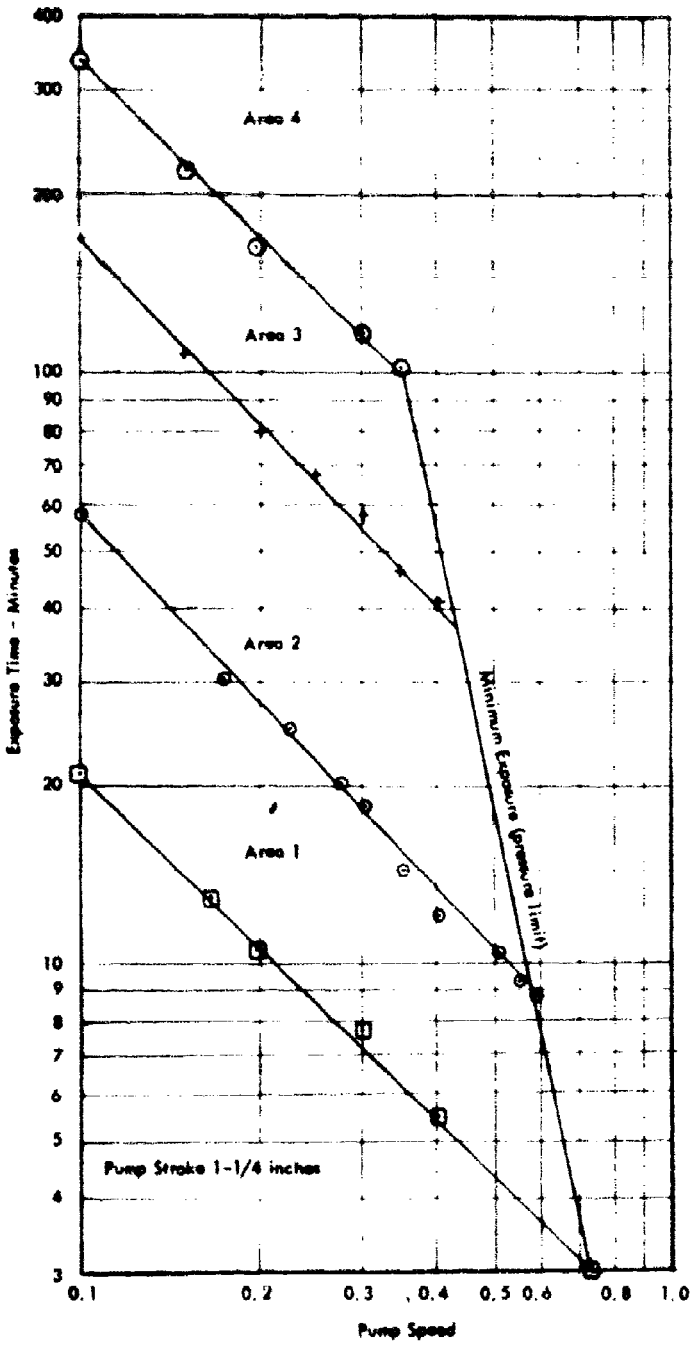

Figure A-2 - Source Field Hydraulic Characteristics

DISTRIBUTION LIST

3 Army Library
CD Unit
Washington, D.C.

1 Assistant Secretary of the Army
R&D
Attn: Assistant for Research
Washington, D.C.

1 Commanding Officer
U. S. Army Nuclear Defense Lab
Attn: Dr. H. Donnert
Army Chemical Center
Edgewood, Maryland

1 Director, U. S. Army Ballistic
Research Lab
Attn: Document Library
Aberdeen Proving Ground, Md.

1 Commanding Officer
U. S. Army Nuclear Defense Lab
Army Chemical Center, Md.

43 Assistant Director for Civil
Defense (Research)
Office of the Secretary of the Army
Pentagon
Washington, D.C.

1 Advisory Committee on Civil
Defense
National Academy of Sciences
Attn: Mr. Richard Park
2101 Constitution Avenue, N. W.
Washington, D.C.

1 Protective Structures Development
Center
Attn: Technical Library
Fort Belvoir, Virginia

1 Chief, Bureau of Yards & Docks
Office of Research, Code 74
Department of the Navy
Washington, D. C.

1 Dr. James O. Buchanan
Director, Shelter Research Div.
Office of Civil Defense, OSA
Department of Defense
Washington, D. C.

20 Defense Documentation Center
Cameron Station
Alexandria, Virginia

1 Director, Defense Atomic Support
Agency
Attn: Technical Library
Washington, D. C.

1 Los Alamos Scientific Laboratory
Attn: Document Library
Los Alamos, New Mexico

1 Director, Oak Ridge National Laboratory
P.O. Box X
Attn: Mr. E. P. Blizard
Oak Ridge, Tennessee

1 Radiation Shielding Information Center
Oak Ridge National Laboratory
P.O. Box X
Oak Ridge, Tennessee

1 Director, Air Force Nuclear Engrg
Facility
Air Force Institute of Technology
Wright - Patterson AFB
Dayton, Ohio

1 Chief of Naval Research, Code 104
Department of the Navy
Washington, D. C.

1 Commanding Officer and Director
Attn: Document Library
U. S. Naval Civil Engineering Lab
Port Hueneme, Calif.

1 Commanding Officer and Director
U. S. Naval Radiological Defense Lab
Attn: Dr. W. P. Kreger
San Francisco, California

1 Commanding Officer and Director
U. S. Naval Civil Engineering Lab
Attn: Dr. C. M. Huddleston
Port Hueneme, Calif.

1 Ottawa University
Department of Physics
Attn: Dr. L. V. Spencer
Ottawa, Kansas

1 University of Illinois
Department of Civil Engineering
Attn: Professor A. B. Chilton
Urbana, Illinois

1 Mr. Charles Eisenhauer
Radiation Theory Section L.3
National Bureau of Standards
Washington, D.C. 20301

1 U. S. Naval Radiological Defense Lab
Attn: Mr. John Dardis
San Francisco, California

1 Chemical Laboratories
Defense Research Board
Attn: Dr. E. E. Massey
Ottawa Canada

1 Chemical Laboratories
Defense Research Board
Attn: Dr. C. E. Clifford
Ottawa, Canada

1 Edgerton, Germeshausen & Grier
Attn: Mr. Z. G. Burson
P. O. Box 1912
Las Vegas, Nevada

1 Director, National Bureau of Standards
Attn: Dr. M. Berger
Washington, D. C. 20301

1 Conesco, Inc.
Attn: Mr. John F. Batter
205 Sixth Street
Cambridge, Mass.

1 Brookhaven National Laboratory
Attn: Document Library
Upton, Long Island, New York

1 Commanding Officer and Director
U. S. Naval Radiological Defense Lab
Attn: Document Library
San Francisco, California 94135